NATIONAL ADVISORY COMMITTEE
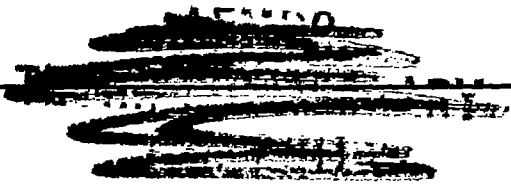# FOR AERONAUTICS

TECHNICAL NOTE 4018

INFLUENCE OF TURBULENCE ON TRANSFER

OF HEAT FROM CYLINDERS

By J. Kestin and P. F. Maeder

Brown University

NACA

Washington
October 1957

NATIONAL ADVISORY COMMITTEE FOR AERONAUT

TECHNICAL NOTE 4018

INFLUENCE OF TURBULENCE ON TRANSFER

OF HEAT FROM CYLINDERS

By J. Kestin and P. F. Maeder

SUMMARY

This report deals with the problem of the influence of free-stream turbulence on the transfer of heat from a cylinder in forced convection at very low Mach numbers but at large Reynolds numbers. In particular, an attempt is made to determine whether the sole influence of turbulence is to shift the point of laminar separation in subcritical flow, or the point of transition in supercritical flow, and thus effect a change in the rate of heat transfer. It is shown that this is not the case and that varying the free-stream turbulence affects local rates of heat transfer.

The results are presented in the form of curves of $\overline{Nu}$ against $\overline{Re}$ and $\overline{St}$ against $\overline{Re}$ (where $\overline{Nu}$ is Nusselt number, $\overline{Re}$ is Reynolds number, and $\overline{St}$ is Stanton number, all based on mean properties); each curve has been plotted for a constant value of turbulence intensity, the temperature effects having been eliminated by the use of integral mean values of the thermodynamic properties of the fluid over the boundary layer. The experimental results unmistakably demonstrate that in the subcritical range the Nusselt number is not independent of the intensity of turbulence.

An attempt to correlate the variation of the Nusselt number at constant Reynolds and Prandtl numbers with the Taylor parameter Λ does not lead to a useful result. Thus, the intensity of turbulence seems to be the primary parameter, at least in the small range of scale values $L = 0.162$ to 0.574 centimeter covered.

This paper presents a survey of related analytical and experimental work and shows that the present tentative conclusions find ample support in previous investigations. It is also pointed out that an oscillation in the free stream has a different effect on the velocity profile and on the temperature profile in the boundary layer which may cause departures from Reynolds analogy, inasmuch as the latter is proved for steady flow only. Hence, it is thought that the Reynolds analogy is a limiting law for zero turbulence intensity.

INTRODUCTION

It has been known for some time that experimental results on the transfer of heat reported by different observers show divergences which exceed the respective experimental errors. It is clear that a systematic influence is at work, and the present report shows that in the range of turbulent flow the structure of the turbulent stream exerts a profound influence on the rate of heat transfer in otherwise similar flows. A dimensional argument of the simplest kind can be used to show that this may be so.

It will be recalled that in the elementary derivation of the laws of similarity which apply in forced convection (refs. 1 to 4) the external flow is always described by specifying only one velocity U_∞, the free-stream velocity. This constitutes an adequate description in cases when the external flow is laminar or, in other words, when its turbulence intensity $\epsilon = 0$. However, when the external flow is turbulent, the laws of similarity imply, in addition, a similarity in the random fluctuations in the streams. Present-day experimental evidence seems to show that an adequate degree of similarity is achieved when the intensity of turbulence

$$\epsilon = \frac{\sqrt{\overline{(u')^2}}}{U_\infty} \tag{1}$$

and the scale of turbulence

$$L = \int_0^\infty G(y)\ dy \tag{2}$$

are fixed in value. Here $\sqrt{\overline{(u')^2}}$ denotes the root mean square of the longitudinal velocity fluctuation, $G(y)$ is the correlation factor

$$G = \frac{\overline{u_1' u_2'}}{\sqrt{\overline{(u_1')^2}}\ \sqrt{\overline{(u_2')^2}}} \tag{3}$$

for fluctuations u_1' and u_2' occurring at a distance y apart. The intensity of turbulence is a measure of the amplitude of the random fluctuations in the stream, and the scale of turbulence serves as a rough measure of the size of eddies present in the stream.

The preceding description of the turbulent free stream disregards the frequency of the random fluctuations, it being implied, as is well known from the Tollmien-Schlichting theory of the origin of turbulence (ref. 5), that the random fluctuations cover a wide range of frequencies of which a given band is amplified at a given Reynolds number

$$Re_\infty = \frac{U_\infty\, d}{\nu} \tag{4}$$

The remaining frequencies are damped out and need not be considered.

A clear understanding of the influence of turbulence on the rate of heat transfer is very important in many engineering applications. It may lead to methods of controlling the rates of heat transfer from solid bodies to fluid streams, whether in the direction of increasing them, for example in boilers or heat exchangers, and thus improving their efficiency or in the direction of reducing them in order to protect the metal walls from deteriorating and burning out at high temperatures. The problem is also important in the calibration of high-temperature probes, inasmuch as the correction factors to be applied to them depend to a great extent on the rate of heat transfer from the stream to the probe.

Probably the greatest experimental effort has been spent in measuring mean coefficients of heat transfer from cylinders in crossflow. This case is, perhaps, not of the greatest importance so far as applications in aerodynamics are concerned, but it constitues the simplest experimental arrangement. Since, in addition, the experimental material available for comparison is abundant, it seems reasonable to begin the investigation with this case.

This investigation has been conducted under the sponsorship and with the financial assistance of the National Advisory Committee for Aeronautics. The authors are indebted to Professor L. S. G. Kovásznay for a very stimulating discussion on the results of the first series of experiments and on the outline of the second series of measurements.

The authors wish to acknowledge the help received from Professor H. H. Sogin of Brown University who performed the second series of measurements and made the corresponding calculations. Messrs. C. C. Cometta and H. E. Wang assisted in the performance of the experiments and helped with the preparation of the diagrams and drawings. Mr. Wang carried out the numerical calculations for the first series and Mrs. J. F. Hall performed the turbulence measurements.

SYMBOLS

A   area of test section

a   thermal diffusivity of fluid

C_b black-body radiation coefficient

C_D drag coefficient

c   correction

c_p specific heat of fluid at constant pressure

d   diameter of cylinder

E   emissivity

G   correlation factor

g   temperature gradient

I   current

I_m measured current

k   thermal conductivity of fluid

L   scale of turbulence

l length of cylinder

l' length of test section

Nu   Nusselt number

$\overline{Nu}$ Nusselt number based on mean properties

P   acoustic pressure

P_{atm} atmospheric pressure

P_b boiler pressure relative to P_{atm}

Pr   Prandtl number

P_s pressure in test section relative to P_{atm}

p pressure

Q quantity of heat transferred

Q_r radiation correction

q dynamic pressure, $\frac{1}{2}\rho V^2$

q_m dynamic head

R resistance

Re Reynolds number

$\overline{Re}$ Reynolds number based on mean properties

R_g gas constant

R_s standard resistance

S frontal area

St Stanton number

$\overline{St}$ Stanton number based on mean properties

s wall thickness

T total temperature

T_{atm} atmospheric temperature

T_m temperature measured in settling chamber

T_o surface temperature of cylinder

T_w temperature of body

T_∞ free-stream temperature

t time.

U potential velocity

U_∞ free-stream velocity

u longitudinal velocity component

u_0 longitudinal velocity component in steady-state solution

u' fluctuating longitudinal velocity component

V voltage

V_m measured voltage

v transverse velocity component

v_0 transverse velocity component in steady-state solution

w velocity

w' measured velocity

w_0 velocity along center line

w_∞ free-stream velocity

x,y coordinates of cylindrical body

α mean coefficient of heat transfer

ϵ intensity of turbulence

θ temperature ratio

Λ Taylor parameter (eq. (6))

λ wavelength of sound wave

μ dynamic viscosity

ν kinematic viscosity

ρ density of fluid

φ angle at which transition occurs on cylinder

ω frequency of oscillation

BACKGROUND OF PROBLEM

A short discussion is now presented of the relationships which must be expected to exist, with the usual assumption that the structure of the turbulence in the external stream may be overlooked, except in the consideration of the position of the point of laminar separation or of the point of transition.

The first question which poses itself is an inquiry into the relation between the purely aerodynamic parameters and the thermodynamic parameters in the flow. It is well known (refs. 5 to 7) that in the range of incompressible flow the temperature field in the stream about a solid body, and hence the mean coefficient of heat transfer, is determined solely by the velocity field when the Prandtl number is constant. On the other hand, the velocity field is independent of the temperature field. Consequently, the Nusselt number $Nu = \frac{\alpha d}{k}$ must be expected to depend on the same parameters as the drag coefficient C_D because the Nusselt number represents an integrated effect of the temperature field and the drag coefficient represents an integrated effect of the velocity field.

It will be recalled that the drag coefficient C_D is a function of one variable, the free-stream Reynolds number Re_∞, in the subcritical and supercritical ranges of Reynolds numbers, whereas in the critical range it also depends on the turbulence of the stream. This may be taken as evidence that the field of flow remains sensibly unaffected by turbulence, except in the critical range, and, by the preceding argument, the same might be expected to be true of the Nusselt number.

As far as can be ascertained, no exact numerical data concerning the overall effect of turbulence on the flow past a cylinder in the range of critical Reynolds numbers are available. However, the problem has been studied with great thoroughness in relation to spheres, notably by Dryden and Kuethe (ref. 8), Dryden (refs. 9 and 10), Dryden, Schubauer, Mock, and Skramstad (ref. 11), and Platt (ref. 12). It was studied with spheres because, before the advent of sensitive and reliable hot-wire anemometers, the turbulence in a tunnel was usually specified by indicating that Reynolds number for which the drag coefficient of a sphere attained the conventional value $C_D = 0.3$. (The lowest value for a sphere is about $C_D = 0.1$, instead of $C_D = 0.36$ for the cylinder.) In the absence of direct measurements on cylinders it is permissible to suppose that the type of relationship to be expected is identical with that for a sphere, the only difference being in the numerical values involved.

The preceding investigations showed that the value of the critical
Reynolds number depends to a marked degree on the intensity and on the
scale of the turbulence in the free stream. However, as shown by Taylor
(ref. 13) and Wieghardt (ref. 14) the critical Reynolds number depends
on the single parameter

$$\Lambda = \epsilon \left(\frac{d}{L}\right)^{1/5} \tag{5}$$

which will be called the Taylor parameter. In order to prove this propo-
sition, Taylor used an argument based on the statistical theory of
turbulence, and Wieghardt used a simplified estimate of orders of mag-
nitude. In both arguments, the essential assumption consists in recog-
nizing that the position of the point of transition is determined by
the turbulent fluctuations in the pressure gradient. The correctness
of this assumption was confirmed experimentally in reference 11 by
showing that the critical Reynolds number is a unique function of the
Taylor parameter Λ from equation (5). The correlation has been made
for spheres of different diameters, all points tracing a single curve
within the experimental error.

There are no reliable data about the angle φ at which transition
occurs on a cylinder at different values of the Taylor parameter Λ,
but it may be noted that transition shifts downstream as Λ is increased.
The critical Reynolds number has a lower value for higher values of Λ,
and, in the case of a cylinder, it ranges from approximately $Re_\infty = 3 \times 10^5$.
at high values of Λ to approximately $Re_\infty = 5 \times 10^5$ at lower values
of Λ.

In an endeavor to determine the independent variables of the prob-
lem, the following view may be taken: The Nusselt number (or the Stanton
number) varies locally around the circumference of the cylinder, its
value at any point being determined by the temperature gradient at the
wall at the point under consideration. In turn, this temperature gra-
dient is determined by the velocity profile, and the velocity gradi-
ent at the wall determines the local coefficient of skin friction. Con-
sequently, the mean Nusselt number could be evaluated if it were pos-
sible to determine the position of the point of separation, laminar or
turbulent, and of the point of transition, if it exists, and if it were
possible to evaluate the local Nusselt numbers from the velocity field.
In addition, it would be necessary to evaluate the variation of the
local Nusselt number in the wake.

From what has been said before it is known that, in the range of
Reynolds numbers where the boundary layer is laminar, the position of the
point of separation is insensitive to the value of the Taylor parameter Λ;
hence, the mean Nusselt number should depend on the Reynolds number alone,
unless the turbulence parameter Λ affects the local temperature gradi-
ent without affecting the velocity profile, or unless it affects the rate

of heat transfer to the wake. Similarly, in the range of Reynolds numbers when the boundary layer is composed of a laminar and a turbulent portion, the mean Nusselt number must be expected to depend on both variables Re_∞ and Λ; for very high Reynolds numbers, when the position of the point of transition and that of turbulent separation cease to be influenced by Λ, the mean Nusselt number must be expected to depend on the Reynolds number alone, unless the structure of the turbulent stream affects the local temperature gradient or the rate of heat transfer in the wake or both.

The present investigation was undertaken with the explicit object of obtaining experimental data against which such conclusions can be tested. In particular, the aim of this investigation is to verify whether the only effect of a variation in the intensity and scale of turbulence is to change the positions of the points of separation and/or the point of laminar-turbulent transition in the flow or whether the change penetrates deeper into the boundary layer thus affecting local values or, in other words, whether it affects the temperature field or the velocity field or both.

Since the aerodynamic aspects of the problem have, so far, been discussed on the basis of experiments with unheated streams it is pertinent to remark here that, strictly speaking, it is necessary to consider an additional similarity parameter, namely

$$\theta = \frac{T_0 - T_\infty}{T_\infty} \tag{6}$$

where T_0 denotes the surface temperature of the cylinder and T_∞ denotes the free-stream temperature. In postulating "incompressible" flow it is implied that the limiting case when the temperature ratio $\theta \to 0$ is being considered. In actual fact, when $\theta \neq 0$, the fluid becomes heated or cooled along its path of flow in the boundary layer, and compressibility effects will manifest themselves even at relatively low speeds.

When presenting experimental data on the transfer of heat between walls and streams it is customary to correct for the influence of this temperature parameter by employing mean values of the properties of the fluid. This aspect of the problem has been thoroughly examined by Humble, Lowdermilk, and Desmon (ref. 15). In the present investigation the influence of the thermal ratio θ on the result has been eliminated by keeping T_∞ and $T_0 - T_\infty$ approximately constant, and integral mean values of the Nusselt number $\overline{Nu}$ and the Reynolds number $\overline{Re}$ have been employed.

It is implied that the discrepancies in the published experimental results on mean coefficients of heat transfer can be traced to the fact that the important influence of turbulence has been neglected. This, of course, is not an omission which can be blamed on negligence. It is due, rather, to the somewhat slow appreciation of the importance of this influence on the flow pattern as well as to the difficulties in measuring the intensity and scale of turbulence under normal experimental conditions and to the practical impossibility of designing an experimental arrangement in which these two parameters could be varied and adjusted continuously in wide limits. As a result, virtually all workers in this field omit furnishing complete descriptions of the structure of the free stream in which experiments have been carried out, and, since this structure was certain to vary in wide limits from investigation to investigation, it is not surprising to discover the existence of serious divergences between sets of data obtained with apparently equal care.

As an example, the data obtained by Hilpert (ref. 16) are compared with those obtained by Griffiths and Awberry (ref. 17) in figure 1. Reference may also be made to the plot on page 259 in reference 4. The spread in the experimental results can be judged by noting the lengths indicating 50- and 100-percent deviations shown in figure 1. This is necessary because the coordinates have been plotted, as usual, on a logarithmic scale. It might be worth noting here that, of the two, Hilpert's stream was undoubtedly the one of lower turbulence intensity, as judged with reference to the descriptions given in references 16 and 17, respectively.

Although it has been known for a long time that a change in the free-stream turbulence affects the rate of heat transfer, no systematic investigations into the details of this influence have been undertaken in the past. Moreover, it is somewhat surprising that current empirical formulas for the relation

$$Nu = f(Re, Pr) \tag{7}$$

tend to effect the correlation for the lowest turbulence intensities. In particular, this is true about Hilpert's (ref. 16) now standard relation for air

$$Nu = A(Re)^m \tag{7a}$$

where the constants A and m vary as the Reynolds number is varied. It might also be noted here that Hilpert's measurements were carried to a Reynolds number $Re = 2.31 \times 10^5$ which was undoubtedly lower than the rather high critical Reynolds number to be expected with his rather low intensity of turbulence.

Reiher (ref. 18) measured Nusselt numbers which were increased by
as much as 50 percent by passing the free stream through a grid placed
upstream of the test tube. Griffiths and Awberry (ref. 17) made meas-
urements on single tubes and tubes arranged in banks. They used a
framework of horizontal wooden laths to increase the turbulence of the
stream in the case of a pipe in longitudinal flow and noticed an increase
in the rate of heat transfer in the upstream portion of the tube of a
magnitude exceeding 100 percent. They made no attempt to determine the
characteristic parameters of either the normal low-turbulence stream or
of the one in which large eddies had been produced, as mentioned. In
performing measurements on square and staggered banks of tubes they
noticed that the downstream rows dissipated heat at a somewhat higher
rate than the front row and ascribed the difference to the presence of
eddies produced by the first row. They also noticed an increase of from
50 to 100 percent in the rate of heat transfer when the free stream was
made turbulent by the framework.

It seems that the first quantitative investigation was carried out
by Comings, Clapp, and Taylor (ref. 19) who measured the influence of
turbulence intensity on the rate of heat transfer from a circular cylin-
der in crossflow but at the lower range of Reynolds numbers (from 400
to 20,000). They found that increased turbulence at a constant Reynolds
number caused a maximum increase of 25 percent in the Nusselt number at
the larger Reynolds numbers, the effect being negligible at the smaller
Reynolds numbers. The intensity of turbulence was measured upstream of
the model with the aid of two hot-wire wake-angle instruments and cor-
rected for diffusion between the measuring station and the model. No
attempt was made to analyze the scale of turbulence. The measurements
were performed in two turbulence ranges: The "lower range" was from
1 to 3 percent; the "higher range" was from 7 to 18 percent. The tur-
bulence generators were made in the form of grids of wooden slats or
dowels whose number, shape, size, and spacing could be varied. The
results obtained in reference 19 are plotted in figures 2 and 3. Fig-
ure 2 represents the effect of turbulence intensity at a Reynolds num-
ber $\overline{Re} = 5,800$ from which it would appear that the turbulence inten-
sity exerts a systematic influence on the Nusselt number provided that
the Reynolds number is high enough, the rate of increase in the Nusselt
number being higher at lower turbulence intensities. Furthermore, the
Nusselt number seems to tend to a definite value as the intensity is
increased.

Figure 3 shows the effect of the Reynolds number at different tur-
bulence intensities. Curve 1 includes points taken at turbulence levels
exceeding 7 percent, curve 2 refers to points taken at turbulence levels
of less than 3 percent, curve 3 shows Reiher's data (ref. 18), and
curve 4 represents the now-standard Hilpert data (ref. 16).

In view of the existence of an analogy between heat and mass trans-
fer, results on the influence of turbulence on mass transfer have some
relevance for the problem in hand. Some measurements of mass transfer

rates were made by Comings, Clapp, and Taylor (ref. 19). More extensive
results (see fig. 4) have been reported by Maisel and Sherwood (ref. 20),
who measured the rate of evaporation of water from cylinders in cross-
flow and from spheres. They measured both the intensity and scale of
turbulence with the aid of a Burgers-Dryden hot-wire anemometer and varied
the eddy structure by the use of two drilled plates provided with a pat-
tern of holes. The turbulence measurements were performed without the
models in the stream. The turbulence intensities varied from 3.5 to
23 percent, the scale varied from 0.51 centimeter to 1.27 centimeters,
and the Reynolds number on the tube varied from 1,000 to about 13,000.

The accuracy of mass transfer measurement is necessarily limited,
and the independent adjustment of intensity and scale of turbulence is
practically impossible. For these reasons the results are somewhat
scattered, but it is worth noting that Maisel and Sherwood found that
the main parameter which influences the rate of mass transfer is the
intensity of turbulence. They do not, however, confirm the type of
relationship obtained by Comings, Clapp, and Taylor. Whereas Comings,
Clapp, and Taylor found a definite flattening of the curve at high tur-
bulence intensities, as shown in figure 2, Maisel and Sherwood obtained
a reversed curvature in the case of spheres, as shown in figure 4.

It might, finally, be mentioned that Williams and Loyzansky and
Schwab measured the influence of turbulence on the transfer of heat
from spheres; however, no access to their reports could be obtained by
the present authors. The results published by Williams and Loyzansky
and Schwab are given in references 20 and 21 and have been plotted as
curves 3a, 3b, and 3c in figure 4.

The preceding review shows that there exist only very preliminary
studies of the effect of turbulence on the transfer of heat in forced
convection. All experimental investigations refer to relatively low
Reynolds numbers below the critical, thus involving only laminar bound-
ary layers and wakes. Moreover, the investigations have been confined
to the measurement of the integrated effect and no attempt has been
made to correlate this effect with the changes affecting the boundary
layer. It is also clear, however, that an exhaustive study of such
effects will require a large amount of experimental work with several
different arrangements.

GENERAL PLAN OF PRESENT INVESTIGATION

As already mentioned, the present investigation is restricted to
the measurement of the overall (mean) coefficients of heat transfer in
crossflow. The structure of the turbulent stream is varied by inserting
suitable screens ahead of the model and by varying their distance from
it.

The experimental program consisted of two series of runs. In the first series, measurements were made on a smooth cylinder in crossflow. In this manner the Nusselt number was affected indirectly by shifts in the points of transition and separation caused by different turbulence intensities as well as directly by the effect of turbulence on local rates of heat transfer. It is, however, clear that the data available in published investigations are inadequate to enable one to determine, first, whether such local effects exist at all and, second, what their magnitude might be. In order to achieve this it would be necessary to possess exact data on local rates of heat transfer from laminar boundary layers, turbulent boundary layers, and wakes in the presence of pressure gradients, as well as precise data on the position of the points of separation, both laminar and turbulent, and on the position of the point of transition.

The second series of runs was designed so as to give a direct answer to the existence of a local influence, without the need to resort to local measurements at this stage. This was achieved by adding two tripping wires to the first tube and by covering the same range of Reynolds numbers and turbulence structures. The addition of tripping wires causes the boundary layer to become turbulent at the wire, provided that the boundary layer is not too stable (that the Reynolds number is not too low). Thus, for a range of Reynolds numbers the point of transition was fixed at the tripping wires and could not be affected by the turbulence in the free stream. In addition, the point of turbulent separation was insensitive to the intensity of turbulence in the free stream, being mainly dependent on the pressure gradient. Consequently, any changes in the rate of heat transfer produced by a change in the turbulence of the approaching stream would have to be interpreted as due to local effects alone, that is, to the influence or turbulence on laminar and/or turbulent boundary layers, as well as on that from the wake, without, however, providing any clues as to which of these influences was the most important one.

EXPERIMENTAL ARRANGEMENT

The measurements were carried out on a single experimental tube made of brass and provided with a highly polished surface. The tube, with an external diameter $d = 10.646$ centimeter, was provided with steam-heated end sections and was formed into a small constant-pressure boiler, similar to the one used by Hilpert (ref. 16). The model was placed normal to the airstream in the test section of the Brown University 22- by 32-inch low-speed wind tunnel in which the airspeed could be varied from 23 to 56 meters per second, thus providing a range of Reynolds numbers $128 \times 10^3 < \overline{Re} < 308 \times 10^3$, where $\overline{Re}$ is based on the mean viscosity of the air across the thermal boundary layer.

For the second group of experiments the tube was provided with two
wires 1/16 inch in diameter soldered along two generators at $\pm 60^\circ$ with
respect to the oncoming stream.

The rate of heat transfer was measured electrically and corrected
for radiation losses. The surface temperature was measured around the
circumference at five points in the median plane with the aid of Chromel-
Alumel thermocouples. A similar thermocouple was used to measure the
stagnation temperature of the stream in the settling chamber of the
tunnel.

The intensity of turbulence and its scale were measured by means
of a two-channel hot-wire anemometer. For the intensity measurements,
only one of the channels was used to measure the magnitude of the tur-
bulence signal caused by the air flowing over a 0.00015-inch-diameter
tungsten wire. The magnitude was obtained by comparing the energy out-
put of the turbulence signal with the output of a square-wave signal of
known input energy.

For the scale measurements, the signals of two wires, which were
independently amplified and compensated, were added or subtracted,
respectively. Thus, the correlation of the two signals for various
distances between wires was obtained and a simple integration then
yielded the turbulence scale.

A more detailed description of the elements of the experimental
arrangement is given as follows.

<center>Wind Tunnel</center>

All measurements were carried out in the Brown University subsonic
wind tunnel. The tunnel (fig. 5) which is of the open-circuit type, is
driven by a 100-horsepower constant-speed motor and is capable of gen-
erating air speeds up to 200 feet per second in the 22- by 32-inch test
section without diffuser. The speed in the test section is adjusted by
varying the pitch of the compressor blades by means of a hydraulic mech-
anism which can be operated while the tunnel is running. In this manner,
speed adjustments within 0.1 millimeter of water column in dynamic pres-
sure are possible. After the air passes through the compressor, it is
decelerated in a diffuser and enters the settling chamber in which a
set of three screens equalizes turbulence fluctuations; it then passes
through the nozzle into the test section. A typical velocity distribu-
tion, as measured in the test section, is shown in figure 6.

The pressure measurements are carried out by means of a double,
Betz type, water micromanometer. This allows a measuring accuracy of
0.1 millimeter of water over a range of 0 to 300 millimeters. Thus,

its relative accuracy for the tests under consideration was of the order of 1 part in 1,000 in dynamic pressure, or 1 part in 2,000 in airspeed measurements. The speed measurement was obtained by careful calibration of the pressure difference between settling chamber and atmospheric pressure, which approximately equals the static pressure in the test section in a free-jet tunnel, against the velocity-distribution measurements by means of a Prandtl tube in the test section.

The free-stream velocity is subject to two principal corrections (ref. 22, pp. 268, 277, and 280), namely, those due to "solid blocking" and to "wake blocking." The solid-blocking correction for a cylinder is given by

$$\beta_{sb} = \frac{\pi^2}{12} \left(\frac{S}{A}\right)^2 \tag{8a}$$

where A denotes the area of the test section and S is the frontal area of the model. The wake-blocking correction is

$$\beta_{wb} = -\frac{1}{4} C_D\left(\frac{S}{A}\right) \tag{8b}$$

where C_D denotes the drag coefficient of the tube and the negative sign occurs because the dynamic head is measured as the difference between the pressure in the settling chamber and that of the atmosphere, that is, far downstream of the model. Consequently,

$$w_\infty = w' \left[1 + \frac{\pi^2}{12} \left(\frac{S}{A}\right)^2 - \frac{1}{4} C_D\left(\frac{S}{A}\right)\right] \tag{9}$$

where w' is the measured velocity and w_∞ denotes the true velocity. The last two terms of the correction cancel each other to a certain extent, and in view of the absence of reliable data on C_D in the region of critical Reynolds numbers no blockage correction was applied. In this case

$$\frac{\pi^2}{12} \left(\frac{S}{A}\right)^2 = 0.0298$$

and $\frac{1}{4} C_D\left(\frac{S}{A}\right)$ varied from 0.0562 at $C_D = 1.18$ to 0.0171 at $C_D = 0.36$, giving a range of correction factors from 0.974 to 1.013. Adopting no correction introduces an average error of 2 percent in the Reynolds number.

In order to correct for the variation in the velocity profile over the model, a uniform correction

$$c = \frac{1}{x_2 - x_1} \int_{x_1}^{x_2} \left(\frac{w}{w_o}\right) dx = 0.9912$$

was applied. Here x_1 and x_2 denote the coordinates of the central section of the test tube measured from the wall, and w_o is the velocity along the center line.

In experiments with the turbulence generators the velocity was determined by the use of a pitot tube placed above the model, and no corrections were applied, which gave a 2-percent accuracy in the Reynolds number.

Hot-Wire Anemometer

The hot-wire anemometer shown in figures 7 and 8 consists of four sections; two are model HWB hot-wire current suppliers and amplifiers from the Flow Corp., and two are turbulence units. These are used in conjunction with an oscilloscope.

For the examination of average and instantaneous velocities a single wire and HWB unit are required. In the correlation measurements involving two wires both HWB units are used, one with each wire. The resultant signals are fed to both turbulence units and the oscilloscope.

The heated wire of the probe responds to the cooling effect of the stream which is a function of its velocity. Since the resistance of the hot-wire is directly related to its temperature, the resistance will be a measure of the velocity. The wire resistance is established through the use of the resistance bridge shown in figure 7. When the bridge is balanced the resistances in the four legs satisfy the relation

$$\text{Wire resistance} = \frac{R_A R_B}{R_R}$$

Operating the wire at a fixed resistance ratio, that is, a fixed ratio of the resistance of the wire heated to the resistance of the wire in equilibrium with the stream, eliminates any significant effect of stream temperature on average velocity measurements.

In order to examine velocity fluctuations, the fluctuating signal across the hot-wire must be amplified in an appropriate manner. Since

the hot-wire response to velocity fluctuations is modified by the heat
capacity of the wire itself, the amplifier contains a circuit which
compensates for the distortion of the signal. This compensating cir-
cuit produces a certain linear combination of the voltage across the
hot-wire and the time rate of change of this voltage, the e being of
equal magnitude at one particular frequency. The attenuator decreases
the input signal to prevent overloading in the amplifier.

A square-wave circuit is used to find the correct value of the
compensation frequency. When a square-wave current passes through the
hot-wire, the resistance of the wire fluctuates, and a distorted volt-
age is fed to the amplifier. It has been shown that, at the proper
frequency, the amplifier output signal will be a square wave. At this
compensation frequency, the output voltage is proportional to the
velocity fluctuations across the wire. The square-wave current also
provides a method for determining the intensity of turbulence, that is,
by a comparison of the velocity signal with that of the square wave.

The output voltages from each of the HWB units, denoted by A and B
in the block diagram of figure 8, are fed to a filter. This filter is
designed to pass only a certain band of frequencies or to pass all fre-
quencies up to a certain limit. In this way high-frequency noise can
be removed for some applications.

A gain control, following the filter circuit and used in combina-
tion with the HWB attenuator, alters the signal to provide considerable
range. Included in the gain circuit is a potentiometer which alters
the gain of the B circuit so as to be identical with the A circuit; this
compensation is necessary because of the differences in wires and vacuum
tubes.

A multiplex circuit provides the following signals: A, -A, B,
and -B, which in the adding circuit are combined to give A alone,
B alone, A + B, and A - B, depending on the position of the selector
switch.

The chosen signal passes through a power amplifier to a bridge cir-
cuit which determines the turbulent energy. In the operation of the
bridge circuit this signal heats a resistor. Wound around this resistor
there is a resistance wire which becomes heated. This heat unbalances
the bridge of which the resistance wire forms a part. The amount of
unbalance, as read on a microammeter, is proportional to the resist-
ance and the temperature of the resistance wire. Because of a linear
relation between the temperature gradient and the rate of heat flow,
the galvanometer reading is proportional to the turbulent energy.

During the measurements great care was taken to keep the wire of
the probe free from dust by frequent cleaning and recalibration.

Model Tube

The design of the test tube (fig. 9) closely follows the one used by Hilpert in his experiments with tubes having larger diameters. It is made in sections 1, 2, and 3. Sections 1 and 2 are end sections provided in order to eliminate axial heat flow. The surface temperature is maintained at a constant level by circulating saturated steam through the end sections at near-atmospheric pressure; the steam is obtained from a small laboratory boiler described later. The pressure in the boiler could be regulated and measured; it did not exceed the atmospheric pressure during a run by more than 20 centimeters of water.

The central section was made of the same brass tube as the end sections. It is shaped into a small boiler and is filled with water which is, in turn, heated with the aid of an immersion heater to which a direct-current adjustable electromotive force is applied. In this manner the Joule heat is transferred radially to the external stream. The interior of the tube communicates with a small water-filled glass U-tube arranged in front of one of the end sections. During a run the voltage applied to the immersion heater is so adjusted as to maintain a constant level of water in the U-tube; consequently, the pressure in the test section is maintained at a constant level during a run and exceeds atmospheric pressure by several millimeters of water. This arrangement prevents the steam from escaping from the test section, and no correction due to condensation or evaporation is required. Thus, by controlling the pressure, a very constant temperature is maintained on the inner surfaces of the walls of the test section.

Before each run, the interior of the test section was carefully purged of air by intensive evaporation through the then empty U-tube. Before a run the U-tube was filled with cold water while the immersion heater was in operation. All protruding parts of the assembly were carefully insulated with cotton wool and aluminum foil. The test section and the end sections were assembled into one unit and machined together, thus insuring that the external surface was cylindrical and smooth. The whole assembly was polished on a lathe and a mirrorlike surface was obtained. The surface was periodically repolished with a brass cleaning compound.

The test section had the following dimensions:

Length, end to end, l', millimeters 508.20
Diameter, d, millimeters 106.46
Wall thickness, s, millimeters 2.72

The mode of assembly is clearly shown in figure 9. It is seen that the end sections are insulated from the test section with the aid of Bakelite spacers which are so shaped as to expose as much as possible of the inner

surface of the tube to the constant-temperature two-phase system in its interior. In evaluating the results, the length of the test section was measured between the center lines of the two spacers and was 509.93 millimeters.

It is clear from the preceding description that during a test run the difference between the pressure of the steam circulating through the end pieces and that prevailing in the test tube did not exceed 60 millimeters of water. This corresponds, at most, to a temperature difference of 0.165° C. Assuming a thermal conductivity of $k = 0.200$ kg-cal/m hr $^\circ$C for the material of the spacers it can be estimated that axial heat flow accounted for, at most, $Q_a = 1.45$ watts per $^\circ$C. Compared with the normal rate of heat transfer of $Q = 1,000$ to $1,500$ watts, the flow of heat in the axial direction is negligible and accounts for, at most, 0.024 percent.

The test tube was provided with five Chromel Alumel thermocouples, arranged as close to the external surface as possible (fig. 10). The thermocouple wire was enameled and only the extreme ends of it were bared. The junctions were soft soldered before the assembly was finally polished. In this way the junctions were both very small and flush with the external surface. They measured an average temperature between the temperatures at a and b as shown in figure 10, the element of brass between them having no effect on the reading.

After completing the first group of experiments, two tripping wires 1/16 inch in diameter were soldered to the tube. The arrangement of the tripping wires is shown in figure 11. The tripping wires were arranged symmetrically, one at 60°, the other at -60° with respect to the oncoming stream.

Boiler and Steam Circulating System

The circulating steam was produced in a small well-insulated boiler (fig. 12) with the aid of three alternating-current immersion heaters. Steam from the boiler passed through the end sections 1 and 2 and through the condenser (d), where it was condensed with the aid of a controlled supply of cooling water. Tube (c) indicated the water level in the boiler, and tube (b) indicated the pressure in its interior. The boiler was operated exclusively on distilled water to prevent scaling.

By suitably adjusting the output from the three main heaters j_1, j_2, and j_3 (1, 2, and 4 kilowatts, respectively) and by adjusting the flow of cooling water with the aid of a needle valve it was possible to attain a steady state of flow under natural circulation. In this way the heat lost by the system by forced convection, by radiation, and to

the cooling water was just balanced by the heat input. The prevalence
of a steady state could be observed with reference to the level in
tube (b). This remained constant within 20 centimeters during a run.

Before a run the air was carefully driven out of the system by
vigorous evaporation and bleeding through a valve in line (g). The
boiler was equipped with a mercury-in-glass thermometer placed in a
pocket which also provided a check on the accuracy of the control.

Electrical Measurements

The electromotive force applied to the immersion heater was gen-
erated at 200 volts direct current with the aid of a rotary converter
set. Since it showed undesirably large fluctuations, a voltage control
and stabilizer was designed and built.

The voltage-stabilizer circuit is shown in figure 13. As seen
from this diagram, approximately 10 percent of the current supplied
to the immersion heater is passed through twelve 6AS7G triodes arranged
by means of two 12AX7 cathode followers, controlled by a stabilized
voltage, to have a constant cathode voltage. The remainder of the
current passes through a hand-operated water-cooled rheostat (15 ohms)
to provide a coarse control of the current.

In this way, the fluctuations of the supply line are reduced to
1 part in 1,000 as was verified with the aid of an oscilloscope. More-
over, the output voltage could be regulated continuously from 90 to
195 volts direct current.

The measuring circuit is shown in figure 14. The electrical
heat Q was obtained by measuring the current and the voltage during
each run, both measurements being performed with the aid of a Leeds
and Northrup type K-2 potentiometer and galvanometer measuring with an
accuracy of 5 in 100,000. The voltage was measured across a fixed
potentiometer consisting of two accurate resistances R_1 = 2,000 ohms
and R_2 = 200,000 ohms. Both resistances were guaranteed by the manu-
facturers to have an accuracy of 0.1 percent and were checked in the
laboratory with the aid of a Leeds and Northrup type 4760 Wheatstone
bridge. In this way

$$V = \frac{R_1 + R_2}{R_1} V_m = 101V_m \tag{10}$$

where V denotes the electromotive force applied and V_m is the elec-
tromotive force measured on the potentiometer. The error in V, as can
be verified easily, was not more than 0.2 percent; the error in V_m
was negligible.

The current I was measured with reference to a Leeds and Northrup
Reichsanstalt type standard resistance R_s immersed in mineral oil.
Since the certificate for the standard resistor was an old one, the
resistance was remeasured with the aid of a Leeds and Northrup type 4760
Wheatstone bridge. It was found that the standard resistance had a
value of $R_s = 0.1001 \pm 0.00005$ ohm at room temperature. Referring
to figure 14 it is seen that

$$I = \frac{V_m'}{R_s} = 9.999 \ V_m' \tag{10a}$$

the accuracy being better than 1 in 1,000.

The total amount of heat transferred

$$Q = VI \tag{10b}$$

is thus seen to have been measured with an accuracy of 0.3 percent.

The current leaking through the fixed potentiometer was of the
order of 0.5 milliampere as compared with a normal current of 12 amperes,
constituting only 0.00004 percent of the total, and could be completely
ignored.

Temperature Measurements

All temperatures were measured with the aid of soldered thermo-
couples made of 0.005-inch-diameter Chromel and Alumel wire. The ther-
mocouple wire was calibrated with the aid of a high-precision Leeds and
Northrup Wenner type potentiometer and with reference to two precision,
etched-stem, mercury-in-glass thermometers (from the Cenco and Taylor
Instrument Companies, respectively) provided with Bureau of Standards
certificates. The accuracy of the calibration was to 0.005° C in the
room-temperature range and to 0.01° C near the steam point.

The cold junction was made by soldering fine enameled copper wires
to the two ends of the thermocouple, so that both measuring leads were
made of copper. The cold junctions were immersed in thin glass tubes
filled with acid-free kerosene. These, in turn, were immersed in a
mixture of finely crushed ice and water accommodated in a Dewar flask
as described by Baker, Ryder, and Baker (ref. 23).

The air temperature was deduced from measurements of the stagna-
tion temperature in the settling chamber of the wind tunnel. This,
in turn, was measured with the aid of an exposed Chromel-Alumel ther-
mocouple placed on a Lucite stem and provided with a reference junction

in the usual way. No radiation correction was considered necessary.
The test-section temperature was calculated from the equation

$$T_\infty = T_m - \frac{w^2}{2c_p} = T_m - \frac{q_m}{\bar{\rho}c_p} \qquad (11)$$

Here T_∞ denotes the free-stream temperature in the test section, T_m
is the temperature measured with the aid of the thermocouple, q_m is
the dynamic heat, $\bar{\rho}$ is the mean air density, and

$$c_p = 0.2405 \text{ kg-cal}/^{\circ}C$$

is the specific heat of air which is assumed constant. Taking a mean
air density of $\bar{\rho} = 1.19$ kilograms per cubic meter gives

$$T_\infty = T_m - 8.13 \times 10^{-3} q_m \qquad (11a)$$

The electromotive force was measured with the aid of a portable
Leeds and Northrup thermocouple potentiometer, model 8662. Measure-
ments were made to 0.12° C so that, consequently, the temperature differ-
ence was known to at least 0.25° C.

As is well known, the five thermocouples arranged circumferentially
in the meridian plane of the test section of the tube would not give
identical indications because the circumferential differences in the
local rate of heat transfer set up different temperature gradients
through the wall of the experimental tube. At the low end of the
Reynolds number range the differences were of the order of 2.4° C and
they decreased to 1.5° C for the highest Reynolds numbers. When cal-
culating the Nusselt number, the arithmetic mean was taken.

Intensity and Scale of Turbulence

As already mentioned, increased turbulence was produced by inserting
screens in the test section of the wind tunnel (fig. 5) and its charac-
teristics were varied by using different screens and by adjusting the
distance from the model. In all, two screens were used as follows:

	Mesh, in.	Diameter of wire, in.	Distance from model, in.
Screen 1	3/4	0.148	12 and 24
Screen 2	1/2	.062	12 and 24

Both screens were used at two distances, 12 and 24 inches, from the center line of the model. In choosing the distances, a compromise had to be struck between the space available and the desire to place the test tube far downstream from the screen in order to reduce the variation in the turbulence intensity between the fore and aft portions of the tube. Furthermore, in order to obtain higher intensities it is necessary to place the screens reasonably close to the model, and some variation in intensity along the path of flow must be tolerated.

It was not considered practicable to perform simultaneous determinations of the Nusselt number and of the intensity and scale of turbulence. Consequently, the tunnel was calibrated for these parameters without the model, measurements having been made at the center line. The value at the center line was then assumed to represent the structure of the turbulent stream with sufficient precision. Measurements were taken at the lowest turbulence obtainable at each tunnel speed, that is, without the turbulence-generating screens as well as with the screens in position.

The quantities measured were the intensity of turbulence referred to the longitudinal (in the direction of the stream) fluctuations u' of the mean velocity U_∞, as given in equation (1), and the scale of turbulence L was obtained by planimetering the respective graphs, representing the variation of the correlation coefficient G with probe separation y as given in equations (2) and (3).

The results of the measurements on turbulence intensity ϵ are shown plotted in figure 15 in terms of the test-section air velocity. When performing the measurements it was noticed that the intensity at a given air velocity decreased as time increased, and it was possible to establish that this effect was due to an accumulation of particles of dust on the main tunnel screen (cf. fig. 5). This effect could not be eliminated under existing conditions, because the tunnel operates on an open circuit in a general engineering laboratory. Consequently, the main tunnel screen was thoroughly vacuum cleaned before the Nusselt number determinations, and the tunnel was calibrated for turbulence intensity. Several check points were taken after the completion of the heat transfer runs.

It is seen from figure 15 that some dust continued to accumulate during the period of time consumed by the Nusselt number determinations. Curve a represents the results obtained in the test section without the screens after vacuum cleaning; curve b gives the results obtained after a period of running and immediately preceding the heat transfer measurements. Two check points obtained with a 5-inch sphere are also shown. Further, curve c has been interpolated through the two check points taken after the completion of the heat transfer measurements. For the final

results, a mean value between curves b and c, curve h, was taken as
being representative of the average running conditions.

Figure 15 also shows curves d and e for screen 1 at 12 and
24 inches, respectively, and curves f and g give the same results for
screen 2. As expected, the accumulation of dust on the tunnel screen
only affected the intensity of turbulence in the test section in the
absence of the turbulence-generating screens. The intensive eddying
produced by the turbulence generators was not measurably affected by
the small changes in the effective mesh of the main screen caused by
the accumulation of fine dust particles. These changes in turbulence
exerted a small influence on the determination of Nusselt numbers and
will be discussed subsequently.

The diagrams showing the variation of the correlation coefficient G
with probe separation y for different screen arrangements are shown in
figure 16. Figure 16(a) shows that, for a given arrangement, the scale
of turbulence is independent of the wind speed inasmuch as the points
taken at 40.4 and 21.8 meters per second with screen 2 at 12 inches from
the test section trace a single curve. As seen from equation (2), the
scale of turbulence L is measured by the magnitude of the area under
the curve. The areas have been measured with the aid of a planimeter,
and the results of the measurements are as follows:

The scale of turbulence for no screen is $L = 0.574$ centimeter;
for screen 1 at 12 inches, 0.234 centimeter; for screen 1 at 24 inches,
0.328 centimeter; for screen 2 at 12 inches, 0.162 centimeter; and, for
screen 2 at 24 inches, 0.173 centimeter.

The maximum influence of the variation of the scale of turbulence
on the Taylor parameter Λ is shown by the ratio

$$\left(\frac{L_{max}}{L_{min}}\right)^{1/5} = \left(\frac{0.574}{0.162}\right)^{1/5} = 1.287$$

This variation is comparatively small so that, consequently, in repre-
senting the experimental results the intensity of turbulence ϵ will
first be used as the main independent variable.

EXPERIMENTAL PROCEDURE AND ACCURACY

(RANGE OF EXPERIMENTS)

In order to minimize the effect of changing turbulence, as described
in the preceding section, the determination of the variation of the

Nusselt number with the Reynolds number was concentrated in a relatively short period of 8 days.

Great care was taken to bleed the system of trapped air, as already mentioned, and suitable precautions were taken to attain thermal equilibrium. At least 30 minutes were allowed to pass before the first readings of a series were taken, that is, when the experiments were started with the facility initially at ambient temperature. When the installation had already been running and only the tunnel speed was changed, it was found that a waiting period of about 15 minutes was adequate.

At each set of operating conditions four complete readings were taken, and a mean value of each measured quantity was used for evaluation. The duration of an average run was 15 minutes, and the following maximum fluctuations at each test point were allowed:

Surface temperature, °C . . . . ±0.05
Air temperature, °C . . . . ±0.07
Current, percent . . . . ±0.4
Voltage, percent . . . . ±0.4
Pressure in test tube, millimeters H_2O . . . . ±60
Boiler pressure, millimeters H_2O . . . . ±200

Table 1 reproduces a typical test run.

The largest single source of error in the determination of the Nusselt number was, as usual, that due to the determination of the temperature difference

$$\Delta T = T_0 - T_\infty \tag{12}$$

where T_0 is the mean surface temperature and T_∞ is the corrected free-stream temperature, as given in equation (11a).

Estimating with the aid of the simple equation

$$Nu = \frac{\alpha d}{k} = \frac{V_m I_m}{\pi L k \ \Delta T} \tag{13}$$

it is found that the Nusselt number was determined with an accuracy of 1 percent.

Similarly, the Reynolds number

$$Re = \frac{wd}{\nu} = C \sqrt{q_m/\rho} \tag{14}$$

where q_m is the dynamic head, $\bar{\rho}$ is the mean density, and C is a numerical constant, was determined with an accuracy of 2 percent.

The first series of tests (smooth tube) consisted of five runs as follows: Run 1.1, no turbulence-producing screens; run 1.2, screen 1 at 12 inches from center line; run 1.3, screen 1 at 24 inches from center line; run 1.4, screen 2 at 12 inches from center line; run 1.5, screen 2 at 24 inches from center line.

The limits of variation of the various parameters were:

Reynolds number, $\overline{Re}$ . . . . 127.8 to 308 × 10³
Nusselt number, $\overline{Nu}$ . . . .   328.8 to 552.4
Intensity of turbulence, percent . . . .   0.68 to 2.67
Scale of turbulence, cm . . . .   0.162 to 0.574

The second series of tests (with tripping wires) also consisted of five runs, numbered 2.1, 2.2, 2.3, 2.4, and 2.5, in exact correspondence with the first series.

The limits of variation of the parameters were:

Reynolds number, $\overline{Re}$ . . . . 133.7 to 315.0 × 10³
Nusselt number, $\overline{Nu}$ . . . .   350.7 to 688.8
Intensity of turbulence, percent . . . .   0.58 to 2.68
Scale of turbulence, cm . . . .   0.162 to 0.574

EVALUATION OF RESULTS

The experimental results were evaluated on the basis of an integrated mean of the properties of air across the boundary layer; that is, for

$$\bar{\nu} = \frac{1}{\Delta T} \int_{T_\infty}^{T_o} \nu \, dt \tag{15}$$

$$\bar{k} = \frac{1}{\Delta T} \int_{T_\infty}^{T_o} k \, dt \tag{15a}$$

The numerical values of $\nu(T)$ and $k(T)$ for air have been interpolated from reference 25. The Prandtl number was constant throughout at

Pr = 0.71 and the gas constant was assumed to be $R_g = 2152.98 \frac{(mm\ Hg)(cm^3)}{(gram)(^oK)}$

as quoted in reference 25.

The radiation correction was calculated from

$$Q_r = EC_b A \left[(T_o/100)^4 - (T_\infty/100)^4 \right] \qquad (16)$$

where the surface area $A = \pi l d$, $C_b = 5.77$ watts/m^2 hr^{o}C^4 (ref. 25)
and the emissivity E was estimated to be E = 0.08. The radiation
correction was at most of the order of 0.8 percent, so that even a
large error in E would exert a negligible influence on the final
result.

The relative humidity varied in the limits of from 30 to 68 per-
cent and was ignored in the evaluation of the results.

EXPERIMENTAL RESULTS FOR FIRST SERIES OF RUNS

The experimental results for the first series of runs are listed
in table 2 and represented graphically in figures 17 to 19. In order
to provide a basis for comparison with Hilpert's data (ref. 16), the
experimental results have been plotted in figure 17 on the basis of
the mean values $\overline{Nu}$ and $\overline{Re}$ as described earlier. Thus, in figure 17
the five runs are represented in terms of $\overline{Nu}$ against $\overline{Re}$ plotted in
logarithmic coordinates and are compared with Hilpert's experimental
points as well as with his interpolation formula

$$\overline{Nu} = 0.0239\ \overline{Re}^{0.805} \qquad (17)$$

for the range $40 \times 10^3 < \overline{Re} < 250 \times 10^3$. The graph in figure 17 also
contains several check points taken after the completion of the main
runs. In this connection it is seen that the low-turbulence data have
become affected by the accumulation of dust on the main wind-tunnel
screen, and curve 1.7 in figure 17 has been interpolated through the
check points. The deviations of the check points from runs 1.2 to 1.5
are too small to warrant further discussion.

The experimental results for run 1.1 are assumed to have been
taken at turbulence intensities which are midway between the values
given by curves b and c in figure 15, and the check points have been
plotted at the values on curve c in figure 15, as the latter two sets
of measurements were taken on two consecutive days.

On examining figure 17 it will be noticed that the present low-turbulence measurements agree tolerably well with Hilpert's data up to a Reynolds number of approximately $\overline{Re} = 175 \times 10^3$, the present values being lower by about 6.7 percent at $\overline{Re} = 200 \times 10^3$.

Figure 18 contains a cross plot of figure 17 and shows the variation of the mean Nusselt number $\overline{Nu}$ with turbulence intensity ϵ at constant Reynolds number $\overline{Re}$. First, it should be noted that the check points, shown at $\overline{Re} = 200$, 190, 180, and 170×10^3, can be extrapolated from the other results with a high degree of precision, thus providing additional proof for the correctness of the reasoning used in this investigation. Second, it is seen that varying the turbulence intensity results in a complex variation in the Nusselt number $\overline{Nu}$ with turbulence intensity ϵ.

The most unexpected result of the present measurements is the presence of rather large variations in the rate of heat transfer for comparatively small variations in turbulence intensity, particularly at the lower end of the scale. This large variation is more pronounced at the lower Reynolds numbers but persists throughout the experimental range; and so, the variation in the rate of heat transfer is of the order of 22 percent at $\overline{Re} = 180 \times 10^3$ for a variation in ϵ from 0.8 to 1.26 percent. The second unexpected result is the presence of a peak in the Nusselt number, which becomes less and less pronounced as the Reynolds number is increased and which, at the same time, shifts toward lower turbulence intensities. It disappears at about $\overline{Re} = 220 \times 10^3$. The presence of the peak gives rise to a range of intensities, different for each Reynolds number, in which an increase in turbulence intensity causes the rate of heat transfer to decrease.

Finally, at higher turbulence intensities, the Nusselt number is seen to increase with turbulence intensity, the rate of increase being approximately independent of the intensity of turbulence at values above about $\epsilon = 2.0$ percent; it should be noted that the curvature of the lines $\overline{Re} = $ Constant changes from concave upwards at $\overline{Re} = 140 \times 10^3$ to convex upwards at $\overline{Re} = 220 \times 10^3$, thus reproducing both types of variation shown in figure 4 and obtained by Comings, Clapp, and Taylor (ref. 19) and by Maisel and Sherwood (ref. 20), respectively. Since the turbulence intensities obtained in the present investigation were much lower than those reported in references 19 and 20 and since the Reynolds numbers were, in turn, higher, no useful comparison can be made at this stage.

It is also noteworthy that the local minimum in the Nusselt number occurs at comparatively high turbulence intensities at lower Reynolds numbers, the minimum point shifting toward lower turbulence intensities

as the Reynolds number is increased. This local minimum disappears at about $\overline{Re} = 220 \times 10^3$, that is, at the same value as the peak mentioned previously.

Table 3 gives an indication of the overall variation in the Nusselt number with turbulence intensity.

The most lucid presentation of the experimental results is given in figure 19, which contains plots of the variation in the Nusselt number $\overline{Nu}$ with the mean Reynolds number $\overline{Re}$ at constant turbulence intensity, together with a comparison with Hilpert's data. It is noteworthy that Hilpert's experimental points, shown separately in figure 19, agree remarkably well with the present result for $\epsilon = 0.90$ percent, even if his interpolation curve, shown as a dashed line, seems to differ in slope from the slightly curved lines representing $\epsilon = 0.85$ and 0.90 percent, respectively.

The variation of $\overline{Nu}$ with $\overline{Re}$ for the lower turbulence intensities cannot be plotted along a straight line in logarithmic coordinates, indicating that the type of variation given in equation (7a) does not hold precisely. It can, however, be approximated by straight lines with a certain loss of accuracy, in which case the exponent m assumed a value which differs somewhat from that found by Hilpert. The same is true about portions of the curves for higher turbulence intensities. Table 4 gives an indication of the values of the exponent m and of the constant A from equation (7a) which may be assumed for different values of intensity of turbulence and in different ranges of Reynolds numbers. It should be noted that in the intermediate ranges of turbulence intensity ($\epsilon = 1.2, 1.3, 1.4, 1.6, 1.8,$ and 2.0) there exists a range of Reynolds numbers over which the exponent m varies rapidly, and the curve cannot be approximated by a straight line in logarithmic coordinates. It seems certain that this corresponds to the critical range of Reynolds numbers.

INFLUENCE OF SCALE OR TURBULENCE AND ROLE

OF TAYLOR PARAMETER

The results shown in figure 18 have been replotted in figure 20, with the intensity of turbulence ϵ being replaced by the Taylor parameter Λ as the independent variable. It is seen that the plots for constant Reynolds number cease to be monotonic and it would appear that at some values of the Taylor parameter Λ there are three corresponding values of the Nusselt number, a result which cannot be accepted on physical grounds. It is suggested that figure 20 shows that the Taylor

parameter cannot be used for the purpose of correlation, as might have been expected from the considerations advanced previously.

DISCUSSION OF RESULTS OBTAINED DURING

FIRST SERIES OF RUNS

The experimental results presented previously support some of the suppositions stated in the "Introduction." There is no doubt about the fact that the structure of the turbulent stream as evidenced by the intensity of turbulence ϵ in a narrow range of variation in the scale of turbulence L exerts a profound influence on the rate of heat transfer, that is, on the Nusselt number. A close examination of table 4 and figure 19 shows that the data obtained by different experimenters do not correlate well enough to fit into one curve or equation and cannot be expected to yield valid results if the important influence of the type of turbulent stream employed is left out of account; this explains the difficulties encountered in past correlations. In particular, referring to Hilpert's very careful measurements (ref. 16), it can be surmised that the intensity of turbulence did not vary considerably in his experimental arrangement and that it was of the order of $\epsilon = 0.85$ to 0.90, since, presumably, the scale of the turbulent stream used by Hilpert was small and not drastically different from that in the present series of experiments.

The important question of the extent of the influence of the turbulence of the stream on the mechanism of heat transfer in particular, and on the boundary layer in general, is best discussed with reference to figure 21 which contains a replot of the data in figure 19 in terms of the variation of the Stanton number $\overline{St}$ with the mean Reynolds number $\overline{Re}$.

A careful examination of the results obtained shows that some curves, for example, the curve for $\epsilon = 1.2$, exhibit unmistakable signs of transition, whereas others, such as $\epsilon = 0.85$ or $\epsilon = 0.90$, lie wholly below the region of transition. On the other hand, the curves corresponding to higher turbulence intensities, such as $\epsilon = 1.5$ and $\epsilon = 2.0$, seem to lie wholly above the transition region. The transition region for $\epsilon = 1.5$ seems to have ended just in the region of its lowest Reynolds number. Evidently, the same conclusions can also be drawn from a scrutiny of figure 19. Further, it is clear from figure 21 that the Stanton number does not exhibit the well-known type of behavior characteristic of the drag coefficient C_D. In particular, the decrease in the Stanton number is smaller than that in the drag coefficient and consequently the rate of change is smaller.

Probably the most interesting feature of the result obtained is the fact that the curves of $\overline{St}$ versus $\overline{Re}$ do not become independent of the intensity of turbulence in the regions below or above the critical value. It will be recalled that the values of the drag coefficient are insensitive to the variation in the Taylor parameter below the critical range of Reynolds numbers. This divergent behavior of the Stanton number, as compared with that of the drag coefficient, would suggest either of the two following conclusions. On the one hand, it is possible that the mean Stanton number is affected to a great extent by the contribution from the wake which may, in turn, depend on the structure of the turbulent stream. On the other hand, it is also possible to suppose at this stage that the variation in the characteristics of the turbulent stream exerts a marked influence on the local temperature profiles.

It is, further, remarkable to note that the use of the Taylor parameter Λ in an effort to account simultaneously for the influence of intensity and scale of turbulence leads to no useful correlation.

It might be useful to recall at this stage that in Hilpert's experiments (ref. 16) it was noticed that the correlation of Nusselt number versus Reynolds number did not plot along one smooth curve but exhibited kinks at certain well-defined Reynolds numbers. This may be explained as follows. It is probable that the turbulence intensity in Hilpert's experimental arrangement varied as the velocity was increased. It will also be recalled that Hilpert covered the wide range of Reynolds numbers by varying the diameter of the tubes and testing each tube over the whole range of velocities. By joining two series of results, the same Reynolds number was obtained with a larger tube diameter and a velocity in the lowest range available and also with a smaller tube diameter and a velocity in the highest range available but with a different turbulence intensity. The difference in turbulence intensities would account for the kink, and it is noteworthy that the kinks did occur at Reynolds numbers at which the tube diameter was changed.

EXPERIMENTAL RESULTS FOR SECOND SERIES OF RUNS

The principal experimental results for the runs with the tripping wires have been collected in table 5. They are seen plotted in figures 22 to 25. Figure 22 represents the variation of the Nusselt number $\overline{Nu}$ with the Reynolds number $\overline{Re}$ for the five runs. The preceding run at tunnel turbulence (that is, without additional screens) has been included for comparison and is shown as a dashed line.

It must be remembered that along each of the curves in figure 22 the turbulence varies in accordance with the calibration given in figure 15. In spite of that, the results are quite revealing. On comparing

runs 1.1 and 2.1 it is seen that the addition of tripping wires has a relatively small effect on the rate of heat transfer at the lower sub-critical Reynolds numbers. Comparing these two runs with run 2.5, it is seen that a change of turbulence intensity from 1.2 to 2.4 percent, as deduced from figure 15 for $\overline{Re} = 140 \times 10^3$, produces a large change in the rate of heat transfer, the Nusselt number being increased by 23 percent. The most important feature of the experimental results is the fact that runs 2.2 to 2.5 with the screens all show higher Nusselt numbers than does run 2.1 without the screens. Thus, an increase in turbulence intensity produces a sizable increase in the Nusselt number on a tube with tripping wires, that is, under conditions in which the point of transition and the point of laminar separation are fixed on the circumference. Hence, it may be concluded that the measured increase in the rate of heat transfer is due to the effect of turbulence on local rates of heat transfer. The overall effect reaches a high value of 26.5 percent at $\overline{Re} = 230 \times 10^3$ for a change in intensity from 0.8 to 2.7 percent.

The diagram in figure 23 contains a cross plot of the results from figure 22. The intensity of turbulence for run 2.1 was determined from the mean curve c of figure 15. It is evident that the accuracy of this cross plot is somewhat reduced from that of figure 22 and it is clear that more points taken at intermediate turbulence intensities would be desirable. However, as is well known, the intensity of turbulence cannot be adjusted independently in a tunnel and a great amount of effort on a trial-and-error basis would be required to obtain a more detailed determination of the curves under consideration. Nevertheless, the main trend in the relationship emerges quite clearly from figure 23. At a constant Reynolds number, the Nusselt number increases with turbulence intensity, the increase being rapid at the lower turbulence intensities and slower at the higher values. Moreover, as the Reynolds number is increased, the range of turbulence intensities over which this rapid increase in Nusselt number takes place is shifted in the direction of lower turbulence intensities.

The variation of the Nusselt number with the Reynolds number at constant turbulence intensity is shown in figure 24, and figure 25 shows the same relation for the Stanton number St. Unlike the results shown in figures 19 and 20 there is now no evidence of transition above $\epsilon = 1.2$ percent, and the experimental results show that the rate of heat transfer increases both with turbulence intensity and with the Reynolds number. The influence of turbulence intensity seems to be somewhat larger at lower Reynolds numbers. For example, at $\overline{Re} = 160 \times 10^3$ an increase in turbulence intensity from $\epsilon = 1.2$ to $\epsilon = 2.6$ percent produces an increase in the Nusselt number from 398 to 505 or 26.9 percent. For the same change in turbulence intensity, at $\overline{Re} = 230 \times 10^3$, the Nusselt number changes from 526 to 646 or by 22.8 percent. The greatest increase in the Nusselt number $\overline{Nu}$, as deduced from figure 23,

ranges from 26.9 percent at $\overline{Re} = 160 \times 10^3$ (ϵ increasing from 0.8 to 2.55 percent) to 22.8 percent at $\overline{Re} = 230 \times 10^3$ (ϵ increasing from 0.58 to 2.68 percent). More detailed results are given in table 6.

The rather large deviation of the curves for $\epsilon = 0.9$, 1.0, and 1.2 percent in figure 24 from the general trend at higher turbulence intensities, particularly at the low Reynolds number end, may be due to the fact that at lower Reynolds numbers and turbulence intensities the laminar boundary layer is very stable, and the tripping wire may not have introduced a sufficiently large disturbance to insure complete transition. It is very difficult to verify such suppositions directly but it is quite certain that at higher Reynolds numbers transition must have been complete, as it occurs even without a tripping wire. Consequently, this possible uncertainty has no effect on the general conclusions drawn in this report.

DISCUSSION AND EXPLANATION

The preceding results provide convincing proof that a change in the intensity of turbulence in the incident stream affects the local rates of heat transfer. On the basis of the present experimental results it is impossible to deduce whether this influence extends over all three regimes of flow around the circumference of the cylinder in the supercritical range, that is, over the laminar boundary layer, over the turbulent boundary layer, and over the wake, or over the two regimes of flow (laminar boundary layer and wake) in the subcritical range. This point can be decided only as a result of local measurements. It is, however, unlikely that the effect does not include the laminar boundary layer, as the succeeding explanation shows.

Since the rate of heat transfer depends exclusively on the temperature gradient at the wall, a change in the turbulence level in the free stream is seen to affect the whole temperature profile across the boundary layer. It is also certain that it affects the velocity profile in view of the coupling between the temperature field and the velocity field as exhibited in the energy equation (ref. 5, p. 256).

A possible theoretical explanation of this effect is that the fluctuations in the velocity in the mean flow are responsible for it. That this must be so emerges from the mere formulation of the mathematical problem of evaluating the effect of a fluctuating free-stream velocity on the boundary-layer profile. No attempt is made to solve this problem, or any related problems, analytically in this paper, but it is possible to demonstrate its essential unity with problems involving oscillations in the free stream.

In trying to understand the present experimental results and in trying to discover the mechanism through which the free-stream fluctuations penetrate across the boundary layer, it is necessary to reexamine some of the fundamental assumptions in boundary-layer theory. Attention is confined to laminar boundary layers because, for them, it is at least possible to formulate the fundamental mathematical problem even if it is difficult to provide a solution.

When a calculation of heat transfer in forced convection is made (see, e.g., ref. 5), the velocity profile in the boundary layer is first determined with the aid of the steady-state boundary-layer equations. The two-dimensional case with parallel mean flow involves the continuity equation

$$\frac{\partial u}{\partial x} + \frac{\partial v}{\partial y} = 0 \tag{18}$$

and the boundary-layer equation

$$u\,\frac{\partial u}{\partial x} + v\,\frac{\partial u}{\partial y} = -\frac{1}{\rho}\frac{dp}{dx} + \nu\,\frac{\partial^2 u}{\partial y^2} \tag{19}$$

Here u and v are the components of the velocity in the boundary layer, x is measured along the cross section of the cylindrical body (assuming that its curvature is gentle), and y is measured at right angles to it. The pressure gradient dp/dx is said to be "impressed" on the boundary layer by the potential external stream, so that

$$-\frac{1}{\rho}\frac{dp}{dx} = U\,\frac{\partial U}{\partial x} \tag{20}$$

The density of the fluid (assumed incompressible) is denoted by ρ, its kinematic viscosity is denoted by ν, and U is the velocity in the external stream, that is, at the outer edge of the boundary layer. In addition, the following boundary conditions are specified:

At $y = 0$, (no slip at wall)

$$u = v = 0 \tag{21}$$

and at $y = \infty$,

$$u = U(x) \tag{22}$$

Having evaluated the velocity profile $u(x,y)$ and $v(x,y)$ the temperature profile may be calculated from the energy equation

$$u \frac{\partial T}{\partial x} + v \frac{\partial T}{\partial y} = \frac{k}{\rho c_p} \frac{\partial^2 T}{\partial y^2} + \frac{\mu}{\rho c_p} \left(\frac{\partial u}{\partial y}\right)^2 \qquad (23)$$

with the boundary conditions at $y = 0$ (body heated to uniform temperature),

$$T = T_w \qquad (24)$$

and at $y = \infty$ (uniform free-stream temperature),

$$T = T_\infty \qquad (25)$$

Here μ, c_p, and k denote the dynamic viscosity, the specific heat at constant pressure, and the thermal conductivity of the fluid, respectively. The body is assumed to be at a constant temperature T_w and the free stream has a constant temperature T_∞. (The group $a = k/\rho c_p$ is the well-known thermal diffusivity of the fluid in the main stream.)

In actual fact, in a turbulent external stream the boundary condition in equation (22) is not satisfied at all because the velocity in the free stream outside the boundary layer fluctuates in a random fashion, so that the equation

$$u = U(x,t) \qquad (26)$$

at $y = \infty$ should be used instead of equation (22). Moreover, turbulent fluctuations cause changes in direction as well as in magnitude, thus modifying the boundary condition at infinity still further. However, this particular aspect is only of secondary importance as far as the present argument is concerned and would tend to complicate it unnecessarily; therefore, it will be assumed that the turbulent fluctuations in the external stream impose a random fluctuation in the magnitude but not in the direction of the mean stream.

Now, since the boundary condition at infinity depends on time, the solution itself will be time dependent, and it is, consistently, necessary to include the time-dependent terms in the differential equations themselves. Thus, equation (19) will be replaced by

$$\frac{\partial u}{\partial t} + u \frac{\partial u}{\partial x} + v \frac{\partial u}{\partial y} = -\frac{1}{\rho} \frac{\partial p}{\partial x} + \nu \frac{\partial^2 u}{\partial y^2} \qquad (27)$$

with the equation of continuity, equation (18), remaining unaltered.
Furthermore, equation (20) will be replaced by

$$-\frac{1}{\rho}\frac{\partial p}{\partial x} = \frac{\partial U}{\partial t} + U\frac{\partial U}{\partial x} \tag{28}$$

The real boundary conditions are given in equations (21) and (26).

Thus, the usual solutions of the steady-state problem are seen to
be valid for the limiting case of

$$\epsilon \rightarrow 0 \tag{29}$$

only, a familiar problem in boundary-layer theory. Namely, it must be
determined whether it is permissible to go over to the limit (eq. (29))
in the differential equations and the boundary conditions or whether
that should be done in the solution itself. The succeeding argument
shows that the two limits are different and that the second course is,
therefore, the right one.

In turbulent flow the velocity component $U(x,t)$ of the potential
velocity oscillates about a mean value $\overline{U(x)}$. Suppose, now, that the
steady-state problem, equations (18) to (23), is solved assuming

$$U(x) = \overline{U(x)} \tag{30}$$

A certain solution (the steady-state solution) will be obtained which
can be denoted by

$$\left.\begin{array}{l} u = u_0(x,y) \\[2mm] v = v_0(x,y) \\[2mm] T = T_0(x,y) \end{array}\right\} \tag{31}$$

Suppose, further, that the full problem, equations (18), (21), (26),
(27), and (28), for the boundary layer is solved. The temperature field
must also now be time dependent, and the energy equation (23) must be
replaced by

$$\frac{\partial T}{\partial t} + u\frac{\partial T}{\partial x} + v\frac{\partial T}{\partial y} = \frac{k}{\rho c_p}\frac{\partial^2 T}{\partial y^2} + \frac{\mu}{\rho c_p}\left(\frac{\partial u}{\partial y}\right)^2 \tag{32}$$

Let this new solution be denoted by

$$
\left.\begin{array}{l}
u(x,y,t) \\[2mm]
v(x,y,t) \\[2mm]
T(x,y,t)
\end{array}\right\}
\tag{33}
$$

It is clear on physical grounds that this solution will also oscillate about a mean which may be denoted by

$$
\left.\begin{array}{l}
u = \bar{u}(x,y) \\[2mm]
v = \bar{v}(x,y) \\[2mm]
T = \bar{T}(x,y)
\end{array}\right\}
\tag{34}
$$

but, because the equations which govern the flow are nonlinear, the solutions in equations (31) and (33) will not be identical; thus,

$$
\left.\begin{array}{l}
u_o(x,y) \neq \bar{u}(x,y) \\[2mm]
v_o(x,y) \neq \bar{v}(x,y) \\[2mm]
T_o(x,y) \neq \bar{T}(x,y)
\end{array}\right\}
\tag{35}
$$

All measurements in a turbulent stream are, evidently, related to the solution $(\bar{u},\bar{v},\bar{T})$, and all solutions with which measurements are normally compared are apparently related to the solution (u_o,v_o,T_o). In questions which involve the transfer of heat the gradient of temperature at the wall $\left(\dfrac{\partial T}{\partial y}\right)_{y=0}$ is of concern but the temperature gradient deduced from the steady-state solution

$$
g_o(x) = \left[\frac{\partial T_o(x,y)}{\partial y}\right]_{y=0}
\tag{36}
$$

will not be identical with that deduced from the time-averaged solution

$$
\bar{g}(x) = \left[\frac{\partial \overline{T(x,y,t)}}{\partial y}\right]_{y=0}
\tag{37}
$$

which corresponds to the measured rate of heat transfer. The two gradients will be identical only in the limiting case $\epsilon \to 0$.

The argument advanced so far shows only that good agreement must not, a priori, be expected between experiment and steady-state theory and that the discrepancy is likely to increase as the intensity of turbulence increases. The next question to be examined concerns the magnitude of this discrepancy. Since, at present, no solution for a single particular case is known in which the temperature profile was given for the full problem, such an estimate cannot be made analytically and thus must be made experimentally. The present two series of experiments show, first, that the mean gradient $\bar{g}$ is greater than its steady-state value g_0 and, second, that at turbulence intensities of the order of 2.6 percent the gradient in equation (37) may exceed that in equation (36) by as much as 25 percent.

In principle, a fluctuating mean stream must also be expected to affect skin friction, as the latter is proportional to the velocity gradient $\left(\dfrac{\partial u}{\partial y}\right)_{y=0}$. It is, however, probably true that this influence is very small; otherwise it would already have been detected by some of the very numerous experimenters in this field. Of this there seems to be no indication at present.

Having noticed the essential difference between the steady-state velocity and temperature fields on the one hand and the mean fields on the other, it may be noted here, parenthetically, that the well-known analogy between heat transfer and skin friction (Reynolds analogy) can now be expected to be true only in the limiting case of $\epsilon \to 0$ because it has been proved on the assumption of steady flow only. The deformation of the velocity profile and the deformation of the temperature profile caused by the fluctuating mean stream cannot be expected to be identical, and, consequently, the Reynolds analogy cannot be expected to be satisfied in the presence of a turbulent main flow. This may explain the difficulties encountered in verifying the Reynolds analogy experimentally. It also seems doubtful that the method of measuring laminar skin friction by measuring rates of heat transfer (ref. 26) will prove reliable, except for very low turbulence intensities.

Apart from causing a deformation in the velocity profile and in the temperature profile, external fluctuations must be expected to give rise to secondary flow in the boundary layer itself. It has been shown by Schlichting (ref. 5, p. 194, or ref. 27) that the combination of nonlinear terms with an oscillation in the stream causes the occurrence of secondary flows in cases for which exact solutions can be obtained, and the same must be expected to be true of the system of equations considered here.

Since in this investigation the view is held that the major influence of turbulence on heat transfer, and possibly also on skin friction,

is due to the fluctuations in the free-stream velocity, it can be seen that several seemingly different problems are closely related to this heat transfer problem. They include the influence of sound fields on heat transfer, the transfer of heat in pulsating flow, and the transfer of heat to oscillating bodies. The latter problem is identical with the general problem because of the well-known equivalence of the equations of motion of an incompressible fluid in systems of coordinates which are in relative (not necessarily steady) motion to each other.

RELATED PROBLEMS

It is doubtful whether the full problem of the influence of turbulence on heat transfer will become amenable to analytical treatment. At the present time no exact solutions of any related problem, even of the simplest kind, are known, but several related investigations both of an analytical and of an experimental nature merit consideration.

Probably the first investigation of secondary motion due to an oscillation is Rayleigh's well-known paper on the circulation of air observed in Kundt's tubes (ref. 28). Rayleigh was already aware of the fact that even when the investigation includes the influence of friction, by which the motion of the fluid in the neighborhood of solid bodies may be greatly modified, there is no chance of reaching an explanation if, as is usual, the investigation is limited by the supposition of infinitely small motion and the squares and higher powers of the mathematical symbols by which it is expressed are neglected.

Rayleigh considered the motion near a solid wall due to a standing wave present in the free stream and was able to demonstrate that the existence of secondary motion ("direct current") is inherent in the Navier-Stokes equations. It is noted that Rayleigh made use of the full Navier-Stokes equations and not of the simplified boundary-layer equations quoted in the preceding section.

A further advance in this direction was made by Schlichting (refs. 5 and 27) who used Prandtl's boundary-layer equations in his calculations. Schlichting obtained a solution for the case when a cylinder (not necessarily circular) oscillates harmonically in a fluid at rest (or when the fluid performs harmonic oscillations about a cylinder). The solution was obtained in the form of a Fourier series expansion of which two terms were calculated by successive approximations. It turns out that even the first approximation shows that at certain instants and at certain points in the boundary layer the velocity actually exceeds the maximum potential velocity (by about 7 percent at most). As expected, the first approximation leads to velocity components in the boundary layer, the time average of which is zero.

The second approximation leads to velocity components which have a steady term and an oscillating term. On taking time averages, the steady terms will give a nonvanishing contribution. This nonvanishing contribution arises because the convective terms in the second approximation lead to expressions which contain squares of trigonometric functions. For example, with

$$U(x,t) = U_1(x) \cos \omega t$$

where U_1 is the amplitude of the velocity of oscillation, the convective term becomes

$$U \frac{\partial U}{\partial x} = U_1 \frac{\partial U_1}{\partial x} \cos^2 \omega t$$

or

$$U \frac{\partial U}{\partial x} = \frac{1}{2} U_1 \frac{\partial U_1}{\partial x} (1 + \cos 2\omega t)$$

From Schlichting's analysis it is, therefore, clear that in order to exhibit the existence of secondary motion it is necessary to take into account the convective terms and to retain terms with double the fundamental frequency, that is, those multiplied by $e^{2i\omega t}$, if the complex notation is used.

The existence of secondary motion has been demonstrated experimentally by Schlichting (refs. 5 and 27) and by Andrade (ref. 29).

Another related problem was recently studied by Lighthill (ref. 30) who considered a main parallel stream performing small harmonic oscillations in magnitude, but not in direction, about a mean value and calculated a first-order approximation to the resulting changes in the laminar boundary layer formed on an infinite cylinder immersed in it at right angles to the stream.

Unlike Schlichting, Lighthill used the system of equations (18), (27), (28), and (32) with the boundary conditions at $y = 0$ (eq. (21)) and at $y = \infty$ (eq. (5a)). For the temperature field he assumed a body of uniform temperature, so that

$$\left. \begin{array}{ll} \Delta T = \Theta & (y = 0) \\ \Delta T \rightarrow 0 & (y \rightarrow \infty) \end{array} \right\} \quad (38)$$

Here, as in equation (32), ΔT denotes the difference between the local temperature and the free-stream temperature, and Θ is a constant.

The fluctuating free-stream velocity has been assumed as

$$V\left(1 + \epsilon e^{i\omega t}\right) \tag{39}$$

where ϵ denotes the amplitude of the oscillation. Hence, Lighthill assumes

$$\left.\begin{aligned} u &= u_0(x,y) + \epsilon u_1(x,y)e^{i\omega t} \\ v &= v_0(x,y) + \epsilon v_1(x,y)e^{i\omega t} \\ U(x,t) &= U_0(x)\left(1 + \epsilon e^{i\omega t}\right) \\ T &= T_0(x,y) + \epsilon T_1(x,y)e^{i\omega t} \end{aligned}\right\} \tag{40}$$

Here u_0 and v_0 are the values of u and v for $\epsilon \to 0$ and thus correspond to those considered in equation (31). For these conditions a first approximation to the solution to order ϵ is obtained. It is easy to see that the omission of terms of order ϵ^2 eliminates from the equations terms multiplied by $e^{2i\omega t}$ which, as explained earlier, give rise to secondary motion. Thus, secondary motions, which may play a crucial part in the calculation of heat transfer, have been excluded by the degree of approximation preserved in reference 30.

Lighthill was able to show that the time-dependent solutions (eqs. (40)) deviate from the quasi-steady profiles which would exist if at any instant t the steady-state boundary-layer equations had been solved for an instantaneous value of the free-stream velocity in equation (39). Moreover, the manner in which the velocity field deviates from its quasi-steady fluctuation is different from the deviation in the temperature field in defiance of Reynolds analogy (ref. (30), p. 2).

The preceding theoretical considerations make it plausible that the observed increase in the rate of heat transfer is mainly connected with secondary motions set up in the boundary layer by the turbulent fluctuations in the external stream.

Apart from the analytical investigations which are related to the problem in hand it is necessary to mention several experimental results. First, it is necessary to mention the well-known increase in the rates of heat transfer observed in pulsating flows through pipes. Second,

experiments on the transfer of heat in fields of sound might be dis-
cussed. The problem of heat transfer in a field of sound was investi-
gated experimentally by Kubanskii (refs. 31 and 32) who measured the
changes in the Nusselt number for a horizontal cylinder placed in a
field of sound radiated from a Hartmann generator (ref. 33). He found
that the Nusselt number increased by 80 percent in natural convection
when the ratio P/λ of the acoustic pressure to the wavelength of the
sound wave increased by a factor of 50. In the case of forced convec-
tion, the Nusselt number increased by 95 percent when the ratio $P/\rho\omega^2$
of the acoustic pressure to the dynamic head of the stream increased
by a factor of 16.

In a more recent investigation, Harrison et al. (ref. 34) measured
the influence of a sound field on the rate of heat transfer to a verti-
cal pipe in the mixed natural and forced convection regime. The meas-
urements show that overall rates of heat transfer increase by about
40 percent in a sound field of an intensity of 140 decibels sound pres-
sure level. It was also shown that local rates increase even more, the
increase reaching values of three times the normal rates in places.

The case of internal flow was recently investigated by Davies and
Al-Arabi (ref. 35) who measured the increase in the rate of heat trans-
fer from a fluid flowing inside the pipe to the walls of the pipe as
various bends, orifices, and sharp edges were placed upstream. They
found that "abnormal turbulence" due to the presence of bends and other
disturbances caused increases in the rate of heat transfer. It is well
known that flow through a bend gives rise to secondary motion (ref. 5).
For this reason it is thought that the experiments performed by Davies
and Al-Arabi give additional support to the statements made in the pres-
ent report.

The increase in the rate of heat transfer in natural convection
due to the oscillation of a cylinder was measured by Martinelli and
Boelter (ref. 36). It was found that the effect depended on frequency
and that above a certain frequency the mean Nusselt number could increase
as much as fivefold. It is quite clear from Schlichting's solution for
an oscillating cylinder that strong secondary currents were present
during the experiment, thus leading to a superposition of forced over
natural convection in agreement with the conclusions reached earlier.
Martinelli and Boelter also made an attempt to obtain an approximate
analytical solution of the related mathematical problem of the transfer
of heat from an infinite vertical plane oscillating vertically.

CONCLUDING REMARKS

The experimental results obtained and the theoretical considera-
tion involved in an investigation of the influence of turbulence on the

transfer of heat from cylinders reveal the need to study the mechanism of flow in, and the mechanism of heat transfer across, boundary layers at the outer edge of which exists a fluctuating velocity. The velocity may fluctuate in an orderly manner, as in pulsating flow, in flow about an oscillating body, or in the presence of an acoustic field. It may fluctuate in a random manner, as in the presence of free-stream turbulence. The oscillation may be purely harmonic, with a well-defined frequency and amplitude, and it may consist of a whole spectrum of amplitudes and frequencies. The latter case cannot be handled simply by superposition because of the essentially nonlinear character of the phenomenon.

Brown University,
      Providence, R. I., March 28, 1956.

REFERENCES

1. Fishenden, M., and Saunders, O. S.:. An Introduction to Heat Transfer.
   The Clarendon Press (Oxford), 1950.

2. Eckert, E. R. G.: Introduction to the Transfer of Heat and Mass.
   First ed., McGraw-Hill Book Co., Inc., 1950.

3. Jakob, Max: Heat Transfer. Vol. I. John Wiley & Sons, Inc.,
   c. 1949.

4. McAdams, William H.: Heat Transmission. Third ed., McGraw-Hill
   Book Co., Inc., 1954.

5. Schlichting, Hermann: Grenzschicht-Theorie. G. Braun (Karlsruhe),
   1951. (Available in English translation as: Boundary-Layer Theory
   (J. Kestin, trans.), McGraw-Hill Book Co., Inc., 1955.)

6. Fluid Motion Panel of the Aeronautical Research Committee and Others
   (S. Goldstein, ed.): Modern Developments in Fluid Dynamics.
   Vol. II. The Clarendon Press (Oxford), 1952.

7. Fluid Motion Panel of the Aeronautical Research Committee and Others
   (L. Howarth, ed.): Modern Developments in Fluid Dynamics, High
   Speed Flow. The Clarendon Press (Oxford), 1953.

8. Dryden, H. L., and Kuethe, A. M.: Effect of Turbulence in Wind
   Tunnel Measurements. NACA Rep. 342, 1930.

9. Dryden, Hugh L.: Reduction of Turbulence in Wind Tunnels. NACA
   Rep. 392, 1931.

10. Dryden, Hugh L.: Turbulence Investigations at the National Bureau
    of Standards. Proc. Fifth Int. Cong. Appl. Mech. (Sept. 1938,
    Cambridge, Mass.), John Wiley & Sons, Inc., 1939, pp. 362-368.

11. Dryden, Hugh L., Schubauer, G. B., Mock, W. C., Jr., and Skramstad,
    H. K.: Measurements of Intensity and Scale of Wind-Tunnel Turbu-
    lence and Their Relation to the Critical Reynolds Number of Spheres.
    NACA Rep. 581, 1937.

12. Platt, Robert C.: Turbulence Factors of N.A.C.A. Wind Tunnels as
    Determined by Sphere Tests. NACA Rep. 558, 1936.

13. Taylor, G. I.: Statistical Theory of Turbulence. V - Effect of Turbulence on Boundary Layer. Theoretical Discussion of Relationship Between Scale of Turbulence and Critical Resistance of Spheres. Proc. Roy. Soc. (London), ser. A, vol. 156, no. 888, Aug. 17, 1936, pp. 307-317.

14. Wieghardt, K.: Über die Wirkung der Turbulenz auf den Umschlagpunkt. Z.a.M.M., Bd. 20, Nr. 1, Feb. 1940, pp. 58-59.

15. Humble, Leroy V., Lowdermilk, Warren H., and Desmon, Leland G.: Measurements of Average Heat-Transfer and Friction Coefficients for Subsonic Flow of Air in Smooth Tubes at High Surface and Fluid Temperatures. NACA Rep. 1020, 1951. (Supersedes NACA RM's E7L31, E8L03, E50E23, and E50H23.)

16. Hilpert, R.: Wärmeabgabe von geheizten Drähten und Rohren im Luftstrom. Forsch. Geb. Ing.-Wes., Bd. 4, Nr. 5, Sept./Oct. 1933, pp. 215-224.

17. Griffiths, Ezer, and Awberry, J. H.: Heat Transfer Between Metal Pipes and a Stream of Air. Proc. Institution Mech. Eng. (London), vol. 125, 1933, pp. 319-382.

18. Reiher, H.: Heat Transfer From Flowing Air to Pipes and Nests of Tubes in Cross Current (Stream Direction at Right Angles to Pipe Axis). Forschungsheft 269, Forsch.-Arb. Geb. Ing.-Wes., 1925, p. 1.

19. Comings, E. W., Clapp, J. T., and Taylor, J. F.: Air Turbulence and Transfer Processes; Flow Normal to Cylinders. Ind. and Eng. Chem., vol. 40, no. 6, June 1948, pp. 1076-1082.

20. Maisel, D. S., and Sherwood, T. K.: Evaporation of Liquids Into Turbulent Gas Streams. Chem. Eng. Prog., vol. 46, no. 3, Mar. 1950, pp. 131-138.

21. Maisel, D. S., and Sherwood, T. K.: Effect of Air Turbulence on Rate of Evaporation of Water. Chem. Eng. Prog., vol. 46, no. 4, Apr. 1950, pp. 172-175.

22. Pope, Alan: Wind-Tunnel Testing. Second ed., John Wiley & Sons, Inc., 1954.

23. Baker, H. Dean, Ryder, E. A., and Baker, N. H.: Temperature Measurement in Engineering. Vol. I., John Wiley & Sons, Inc., 1953.

24. Hilsenrath, Joseph, Beckett, Charles W., Bendict, William S., et al.:
    Tables of Thermal Properties of Gases. Circular 564, Nat. Bur.
    of Standards, U. S. Dept. Commerce, Nov. 1, 1955.

25. Schmidt, E. (J. Kestin, trans.): Thermodynamics: Principles and
    Applications to Engineering. The Clarendon Press (Oxford), 1949.

26. Ludwieg, H.: Ein Gerät zur Messung der Wandschubspannung turbulenter
    Reibungsschichten. Ing.-Arciv, Bd. 17, Heft 3, 1949, pp. 207-218.

27. Schlichting, H.: Calculation of Periodic Two-Dimensional Boundary
    Layer Flows. Phys. Zs., vol. 33, no. 8, 1932, pp. 327-335.

28. Rayleigh, Lord: On the Circulation of Air Observed in Kundt's Tubes
    and On Some Allied Acoustical Problems. Phil. Trans., vol. 175,
    pt. 1, 1884, pp. 1-21.

29. Andrade, E. N. da C.: On the Circulations Caused by the Vibration
    of Air in a Tube. Proc. Roy. Soc. (London), ser. A, vol. 134,
    no. 824, Dec. 2, 1931, pp. 445-470.

30. Lighthill, M. J.: The Response of Laminar Skin Friction and Heat
    Transfer to Fluctuations in the Stream Velocity. Proc. Roy. Soc.
    (London), ser. A, vol. 224, no. 1156, June 9, 1954, pp. 1-23.

31. Kubanskii, P. N.: Techenia u nagretovo tverdovo tela v stoiachei
    akusticheskoi volne. Zhurnal Tekhnicheskoi Fiziki, vol. 22, no. 4,
    1953, pp. 585-592. (Available in English translation as: Flow
    Near a Heated Solid Body in a Standing Acoustic Wave. LAL, NACA,
    Oct. 1955.)

32. Kubanskii, P. N.: Vliiani akusticheskikh kolebanii konechnoi
    amplitudi na progranichnii sloi. Zhurnal Tekhnickeskoi Fiziki,
    vol. 22, no. 4, 1952, pp. 593-601. (Available in English trans-
    lation as: Effect of Acoustical Vibrations of Finite Amplitude
    on the Boundary Layer. LAL, NACA, Oct. 1955.)

33. Hartmann, J.: The Acoustic Air-Jet Generator. Ingenirvidenskabelige
    Skrifter, no. 4, 1939.

34. Harrison, W. B., Boteler, W. C., Jackson, T. W., Lowi, A., Jr., and
    Thomas, F. A., Jr.: Heat Transfer to Vibrating Air Columns.
    Contract NAw-6400, NACA and Ga. Inst. of Tech., Dec. 1955.

35. Davies, V. C., and Al-Arabi, M.: Heat Transfer Between Tubes and
    A Fluid Flowing Through Them With Varying Degrees of Turbulence
    Due to Entrance Conditions. Chartered Mech. Eng., vol. 2, no. 3,
    Mar. 1955, pp. 150-151.

36. Martinelli, R. C., and Boelter, L. M. K.: The Effect of Vibration
     on Heat Transfer by Free Convection From a Horizontal Cylinder.
     Proc. Fifth Int. Cong. Appl. Mech. (Sept. 1938, Cambridge, Mass.),
     John Wiley & Sons, Inc., 1939, pp. 578-584.

TABLE 1

TYPICAL TEST RUN

$$\left[P_{atm} = 757 \text{ mm Hg}; \ q_{settling} = 63 \text{ mm H}_2\text{O}; \ q_{test} = 40 \text{ mm H}_2\text{O};\right.$$
$$\left. T_{atm} = 23 \text{ }^\circ\text{C}; \text{ relative humidity, } 55 \text{ percent} \right]$$

Run	T_0, $^\circ$C	T_1, $^\circ$C	T_2, $^\circ$C	T_3, $^\circ$C	T_4, $^\circ$C	T_5, $^\circ$C	I_m, amp	V_m, v	P_s, mm	P_b, mm	Time, hr:min
1	4.105	4.08	4.10	4.11	4.11	1.04	11.511	116.64	20	120	10:33
2	4.11	4.08	4.11	4.11	4.11	1.05	11.459	116.12	35	100	10:36
3	4.11	4.08	4.11	4.11	4.11	1.05	11.465	116.10	32	100	10:40
4	4.11	4.075	4.11	4.11	4.11	1.05	11.465	116.11	33	100	10:42

TABLE 2

EXPERIMENTAL RESULTS FOR FIRST SERIES OF RUNS

Run	P_{atm}, mm Hg	T_0, °C	T_∞, °C	U_∞, m/sec	$\overline{Re}$	$\overline{Nu}$	$\overline{St}$
1.1	772.2	99.89	21.51	24.83	141.4×10^3	238.8	3.275×10^{-3}
	772.0	99.89	22.08	27.86	158.5	352.4	3.131
	772.2	99.98	22.96	31.12	176.6	386.9	3.086
	772.1	99.52	23.82	34.07	193.1	410.4	2.993
	771.9	99.52	23.98	37.01	209.7	433.0	2.908
	766.5	99.29	25.14	38.69	217.2	438.0	2.840
	766.4	99.41	25.88	40.16	224.9	445.1	2.787
	766.2	99.54	26.30	41.72	233.2	449.5	2.715
	765.8	99.50	26.38	43.67	244.0	449.9	2.597
	765.5	99.32	26.79	45.87	256.0	453.2	2.493
	765.1	99.28	26.98	47.62	265.5	456.8	2.423
	764.8	99.40	27.24	48.48	269.9	457.1	2.385
	764.5	99.54	27.51	49.34	274.3	460.9	2.367
	764.5	99.54	28.00	50.99	283.2	474.1	2.358
	764.5	99.25	28.62	52.61	291.9	499.9	2.412
	764.5	99.37	28.64	53.37	296.1	514.5	2.447
	764.4	99.25	29.51	55.68	308.3	544.1	2.486
1.2	757.3	99.25	25.10	23.06	127.9	365.1	4.021
	757.0	99.55	25.77	25.81	142.7	391.2	3.861
	757.0	99.32	26.01	28.57	158.0	414.6	3.696
	756.8	99.32	26.51	31.90	176.2	443.3	3.544
	756.8	99.37	26.78	34.91	192.6	467.5	3.419
	756.7	99.48	27.25	38.17	210.3	490.5	3.285
	756.5	99.30	27.98	40.93	225.1	512.9	3.209
	754.3	99.18	32.74	43.32	234.8	528.3	3.169
1.3	768.0	99.18	24.05	23.21	130.9	371.9	4.002
	767.8	99.10	24.72	25.58	144.0	388.3	3.798
	767.8	99.13	25.46	28.34	159.3	406.9	3.598
	767.8	99.40	26.43	31.67	177.4	429.5	3.410
	767.8	99.60	26.87	34.66	193.9	447.9	3.253
	767.8	99.47	27.42	37.65	210.4	466.9	3.126
	767.8	99.70	28.95	40.69	226.3	489.6	3.047
	767.8	99.70	29.47	42.71	237.3	502.0	2.980
1.4	766.5	99.40	26.70	24.03	134.3	386.8	4.057
	756.3	99.15	24.71	26.41	146.5	409.2	3.934
	766.5	99.35	27.22	28.45	158.8	429.0	3.805
	761.4	99.25	22.96	31.62	177.3	444.6	3.532
	760.9	99.42	24.84	34.70	193.4	454.4	3.309
	760.5	99.37	25.03	37.68	209.7	469.5	3.153
	759.0	99.38	24.60	40.63	226.0	483.1	3.011
	756.3	99.18	25.34	42.35	234.5	494.8	2.972
	759.0	99.40	24.82	43.76	243.3	504.9	2.923
1.5	756.0	99.35	24.01	23.03	127.8	362.1	3.991
	756.0	99.32	23.96	25.75	143.0	381.9	3.761
	760.0	99.32	24.13	28.42	158.6	405.6	3.602
	760.0	99.25	24.42	31.72	176.9	430.3	3.426
	756.0	99.15	24.94	33.36	184.9	444.9	3.389
	756.0	99.28	24.81	34.81	192.9	454.2	3.316
	765.5	99.60	25.69	37.60	210.3	481.6	3.225
	756.0	99.25	25.15	37.80	209.2	474.8	3.197
	765.6	99.57	23.87	40.40	227.0	504.3	3.129
	765.6	99.67	25.02	43.96	246.3	528.0	3.019
	765.6	99.65	26.09	47.27	264.2	552.4	2.945

0

TABLE 3

CHECK POINTS FOR EXPERIMENTAL RESULTS OF TABLE 2

Run	P_{atm}, mm Hg	T_O, °C	T_∞, °C	U_∞, m/sec	$\overline{Re}$	$\overline{Nu}$	$\overline{St}$
1.1	765.3	99.52	25.37	35.95	201.3×10^3	403.6	2.824×10^{-3}
	765.3	99.52	24.56	31.08	174.4	366.1	2.957
	761.5	99.28	23.01	45.26	253.7	446.8	2.480
	761.5	99.48	24.00	53.07	296.7	501.6	2.381
1.2	760.0	99.50	23.13	25.80	144.2	399.9	3.906
	760.0	99.38	23.63	40.34	225.3	520.9	3.256
1.3	760.0	99.50	23.51	40.53	226.4	489.3	3.044
	760.0	99.42	23.63	25.98	145.1	388.2	3.768
1.4	760.0	99.42	22.83	26.26	147.0	414.7	3.973
	760.0	99.47	23.15	40.50	226.5	488.1	3.035
1.5	761.3	99.60	22.89	25.61	143.4	386.4	3.795
	761.3	99.40	23.50	40.49	226.6	503.5	3.130
	765.3	99.70	25.69	30.36	169.7	427.1	3.545
	765.3	99.67	25.65	31.68	177.2	435.5	3.461

NACA TN 4018

TABLE 4

OVERALL VARIATION OF NUSSELT NUMBER WITH TURBULENCE INTENSITY

Re	Turbulence intensity, ϵ, percent		Mean Nusselt number, $\overline{Nu}$		Overall percentage variation in Nusselt number, referred to lower value, percent
	Lowest	Highest	Lowest	Highest	
140×10^3	0.87	2.38	325	385	18.4
150	.84	2.47	342	401	17.2
160	.81	2.55	358.5	417	16.3
170	.78	2.62	375	432	15.2
180	.78	2.62	391	447	14.3
190	.72	2.67	407.5	462	13.3
200	.68	2.64	421	477	13.3
210	.66	2.64	433	491	13.4
220	.63	2.66	441	506	14.7

TABLE 5

CONSTANTS IN EQUATION $\overline{Nu} = A \ \overline{Re}^{m}$ IN TERMS OF

TURBULENCE INTENSITY AND REYNOLDS NUMBER

ε, percent	m	A	$\overline{Re}$
0.85	0.890	0.0085	140 to 210 × 10³
.90	.857	.0129	140 to 210
	.862	.0101	140 to 160
1.0 {	.684	.108	160 to 190
	.620	.236	190 to 210
	.553	.546	140 to 170
2.2 {	.625	.230	170 to 210
2.4	.592	.345	140 to 210
2.6	.585	.380	160 to 210

TABLE 6

EXPERIMENTAL RESULTS FOR RUNS 2.1 TO 2.5 WITH TRIPPING WIRES

Run	P_{atm}, mm Hg	T_0, °C	T_∞, °C	U, m/sec	$\overline{Re}$	$\overline{Nu}$	$\overline{St}$
2.1	762.0	99.5	26.24	25.04	139.3×10^3	350.7	3.546×10^{-3}
	762.0	99.6	25.60	28.21	157.5	404.0	3.614
	760.0	99.6	25.96	34.48	191.5	459.3	3.377
	758.9	99.7	26.88	38.99	215.7	497.3	3.248
	758.6	99.7	28.28	48.77	268.6	592.2	3.105
	756.2	98.0	29.58	42.66	234.5	533.4	3.204
	756.2	98.0	28.99	46.32	255.0	574.0	3.171
	755.3	95.8	31.20	55.44	304.9	687.3	3.176
	755.3	96.0	29.29	52.33	288.9	662.3	3.229
	755.3	98.58	26.29	31.36	173.4	426.9	3.468
	776.3	101.70	26.80	25.06	133.7	354.6	3.736
	776.3	99.52	28.45	45.65	257.5	579.1	3.167
	776.3	98.98	27.69	47.32	267.7	607.8	3.198
	776.3	99.93	27.16	48.95	276.6	619.3	3.153
	776.3	98.78	27.90	50.61	286.4	646.4	3.179
	776.8	99.13	30.09	52.33	294.2	654.7	3.134
	776.9	99.08	30.35	53.86	302.7	670.7	3.121
	776.9	99.08	30.18	56.01	315.0	688.8	3.080
2.2	761.0	99.50	27.85	24.30	134.4	434.9	4.557
	761.0	99.40	30.35	30.41	167.3	520.5	4.382
	761.0	99.40	29.71	34.98	192.8	562.8	4.111
	761.0	99.40	31.29	42.05	230.8	651.6	3.976
	760.8	99.35	25.44	26.05	145.1	471.8	4.580
	760.8	99.35	26.59	28.24	156.8	497.7	4.470
	761	99.30	28.79	32.71	180.8	550.4	4.288
	761.3	99.13	28.96	38.34	212.0	613.8	4.878
2.3	769.3	99.89	26.63	24.33	136.5	418.4	4.316
	769.3	99.70	28.58	30.16	168.4	483.0	4.040
	769.3	99.42	29.70	36.42	202.9	554.2	3.847
	769.3	99.67	29.67	42.09	234.4	609.3	3.661
2.4	772.0	98.88	27.46	24.65	138.8	426.5	4.327
	772.0	98.36	28.34	30.09	169.3	495.8	4.125
	771.4	98.14	28.13	36.28	204.2	567.7	3.916
	771.4	98.84	28.59	45.35	254.4	656.5	3.635
2.5	774.2	99.67	26.94	24.66	139.1	409.7	4.148
	774.2	99.23	27.94	30.03	169.2	474.6	3.951
	771.2	98.51	28.92	30.13	169.0	473.3	3.944
	774.1	98.76	27.81	36.19	204.2	546.0	3.766
	774.1	99.18	27.90	45.23	254.9	631.1	3.487

TABLE 7

MAXIMUM EFFECT OF TURBULENCE ON NUSSELT NUMBER

$\overline{Re}$	ϵ, percent		$\overline{Nu}$		Increase in $\overline{Nu}$, percent
	Lowest	Highest	Lowest	Highest	
140×10^3	0.87	2.37	362.0	455.5	25.8
150	.84	2.46	380.5	481.5	26.5
160	.80	2.55	398.5	505.5	26.9
170	.78	2.61	416.5	527.5	26.7
180	.74	2.66	434.5	547.5	26.0
190	.72	2.67	453.0	568.0	25.4
200	.67	2.64	471.0	588.0	24.8
210	.64	2.64	489.0	607.5	24.2
220	.62	2.66	507.5	627.0	23.5
230	.58	2.68	527.0	646.0	22.8
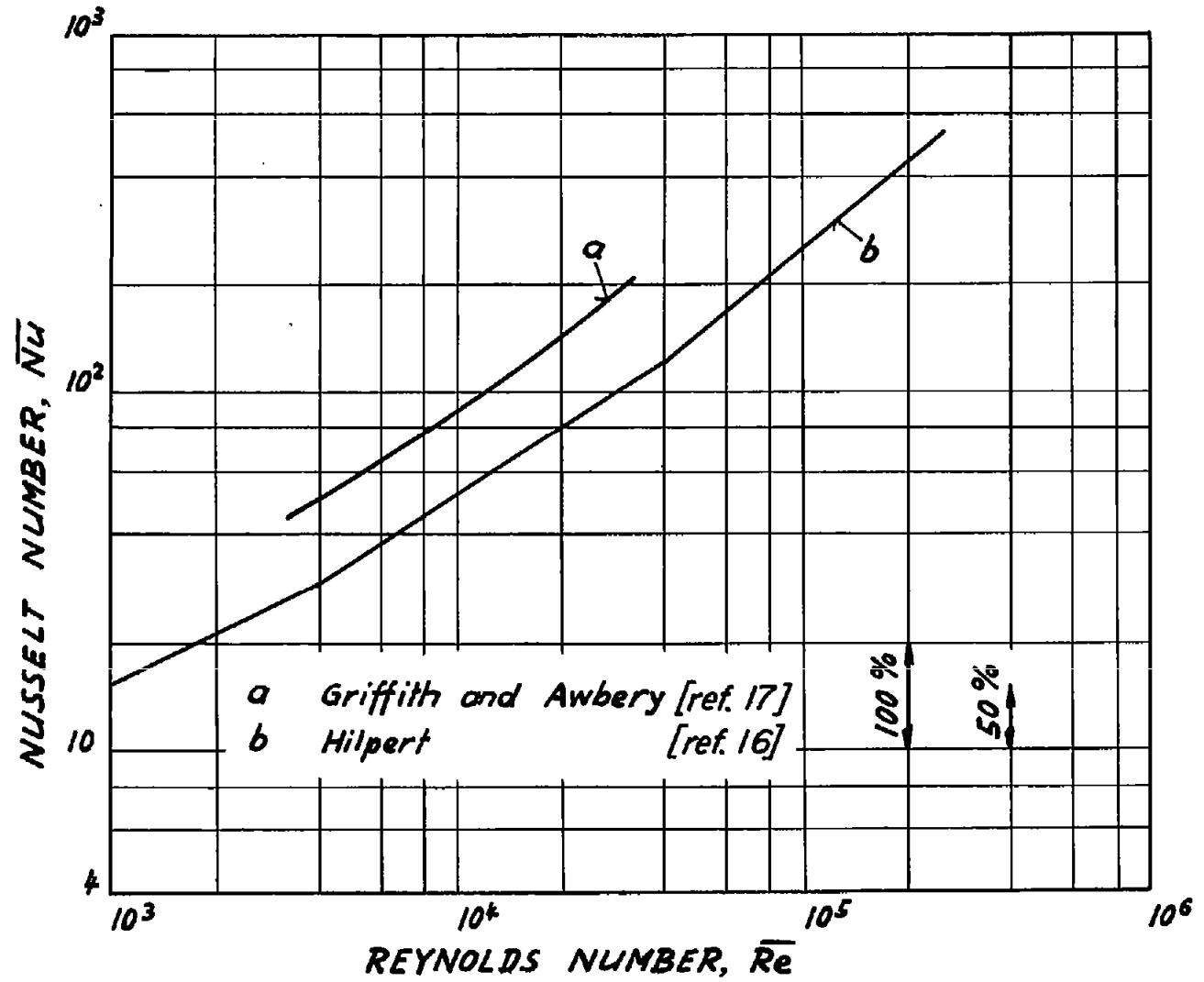
Figure 1.- Comparison between Hilpert's measurements and those made by Griffith and Awbery.
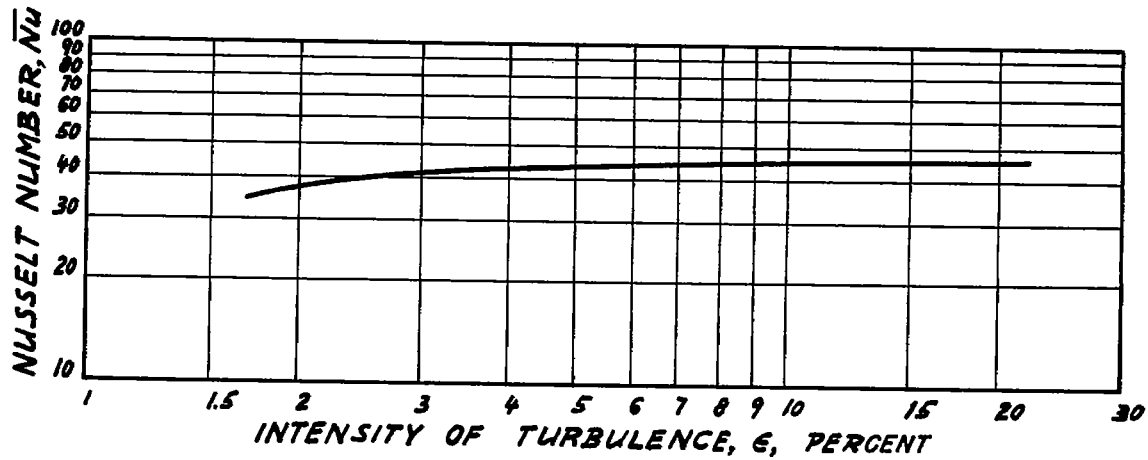
Figure 2.- Effect of turbulence on heat transfer as measured by Comings, Clapp, and Taylor (ref. 19). $\overline{Re}$ = 5,800.
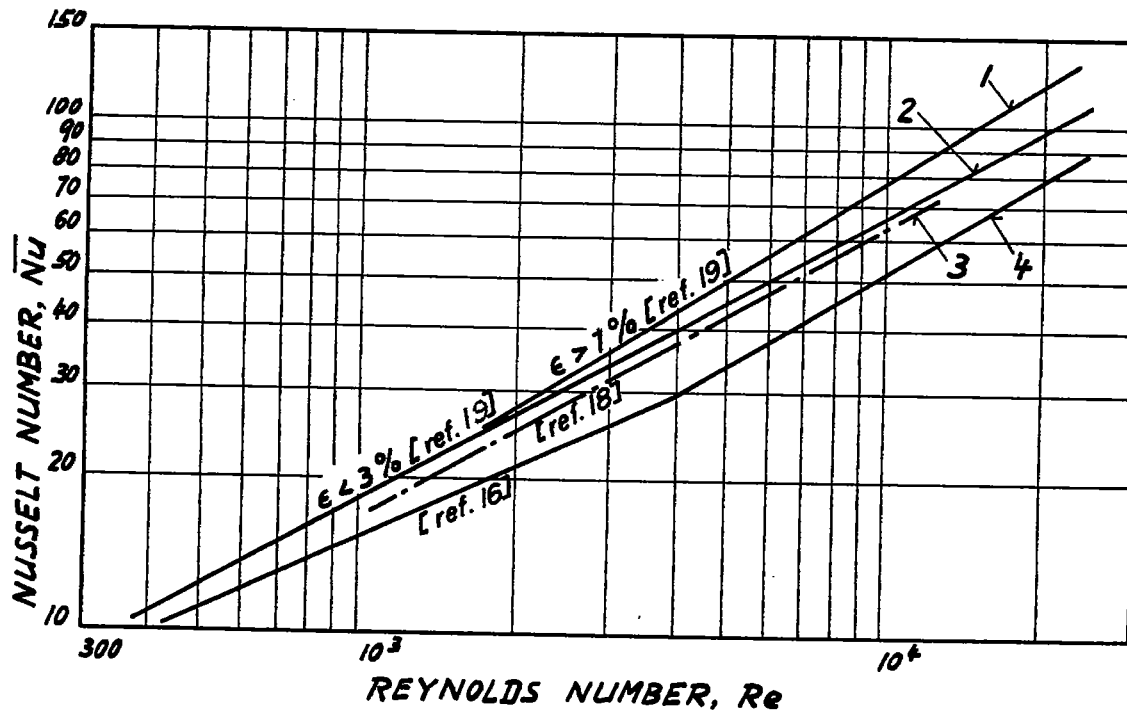
Figure 3.- Effect of turbulence on heat transfer as measured by Comings, Clapp, and Taylor (ref. 19) compared with that measured by Hilpert (ref. 16). Curve 1 includes points taken at turbulence levels exceeding 7 percent, curve 2 refers to points taken at turbulence levels of less than 3 percent, curve 3 shows Reiher's (ref. 18) data, and curve 4 represents the now-standard Hilpert data (ref. 16).
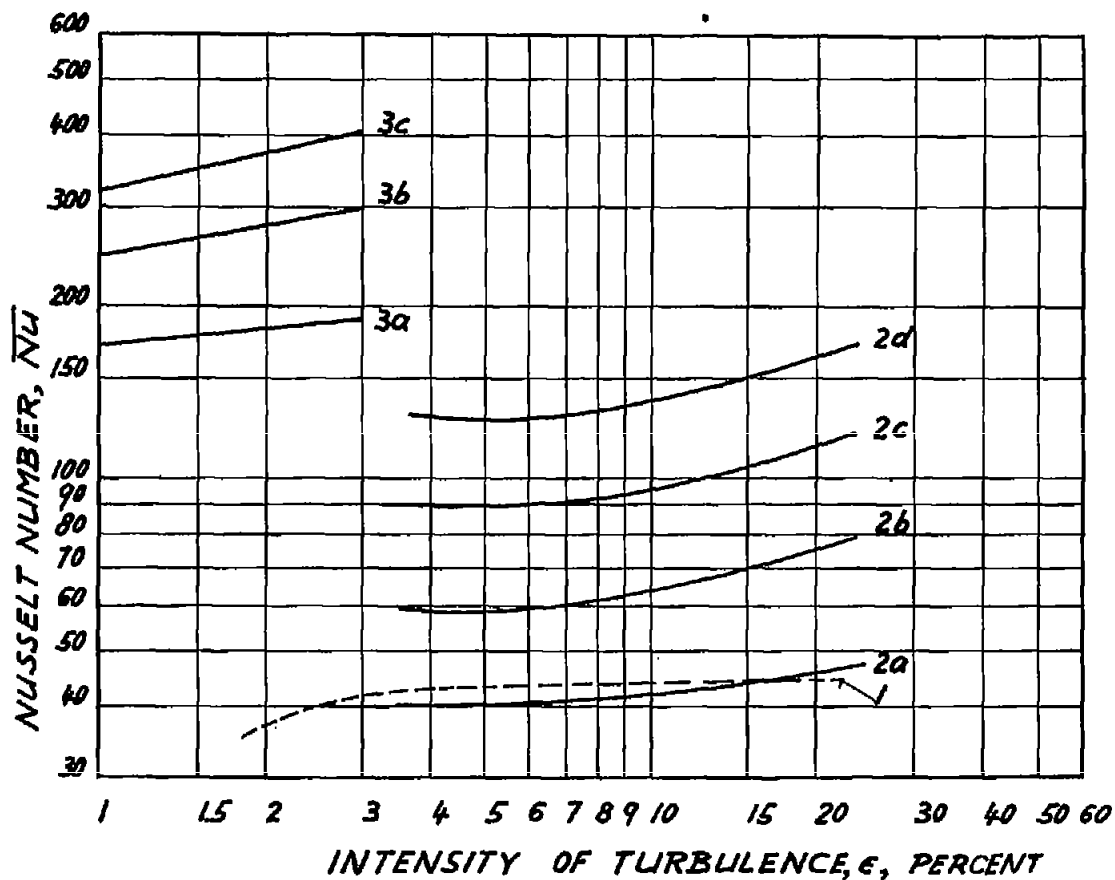
Figure 4.- Effect of turbulence intensity on mass transfer coefficients for spheres, as obtained by Maizel and Sherwood (refs. 20 and 21), compared with data presented in figure 2 and with results obtained by Williams and Loyzansky and Schwab (given in refs. 20 and 21) on transfer of heat from spheres. Explanation of curve labels: 1, curve from figure 2; 2, results obtained by Maizel and Sherwood on spheres for a, $\overline{Re} = 2{,}440$; b, $\overline{Re} = 6{,}060$; c, $\overline{Re} = 12{,}450$; and d, $\overline{Re} = 19{,}500$; 3, results obtained by Loyzansky and Schwab for a, $\overline{Re} = 4 \times 10^5$; b, $Re = 8 \times 10^5$; and c, $Re = 12 \times 10^5$.
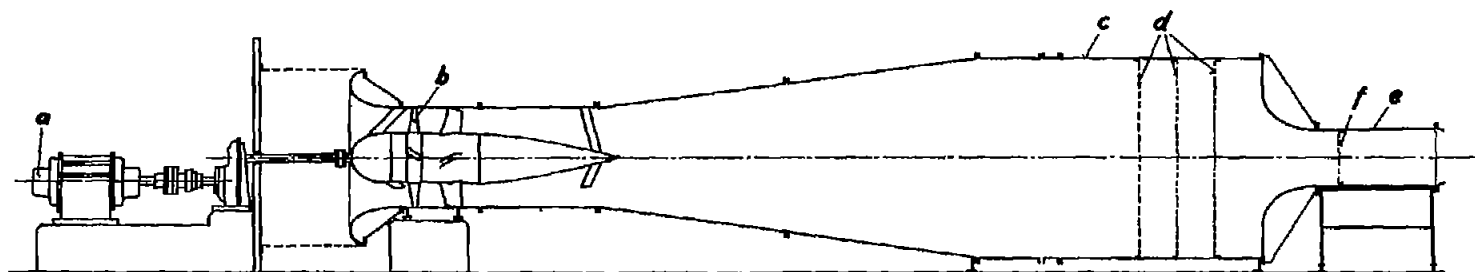
Figure 5.- Layout of Brown University 22- by 32-inch low-speed wind tunnel. Labels indicate:
a, electric motor; b, fan (adjustable pitch blades); c, settling chamber; d, screen; e, test
section; and f, turbulence screen.
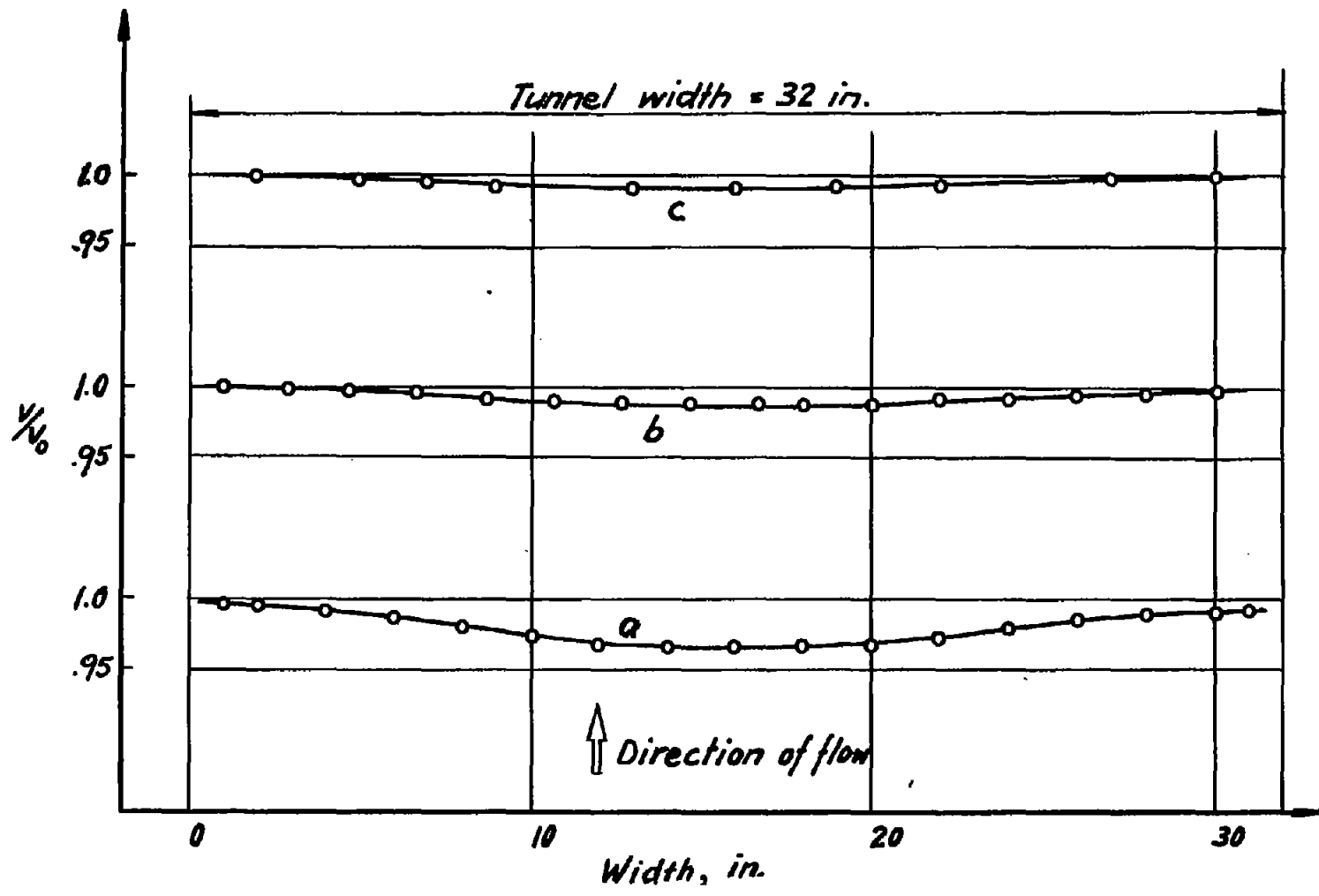
Figure 6.- Velocity distribution in test section of wind tunnel. Labels indicate: a, beginning of test section; b, center of test section; and c, end of test section.
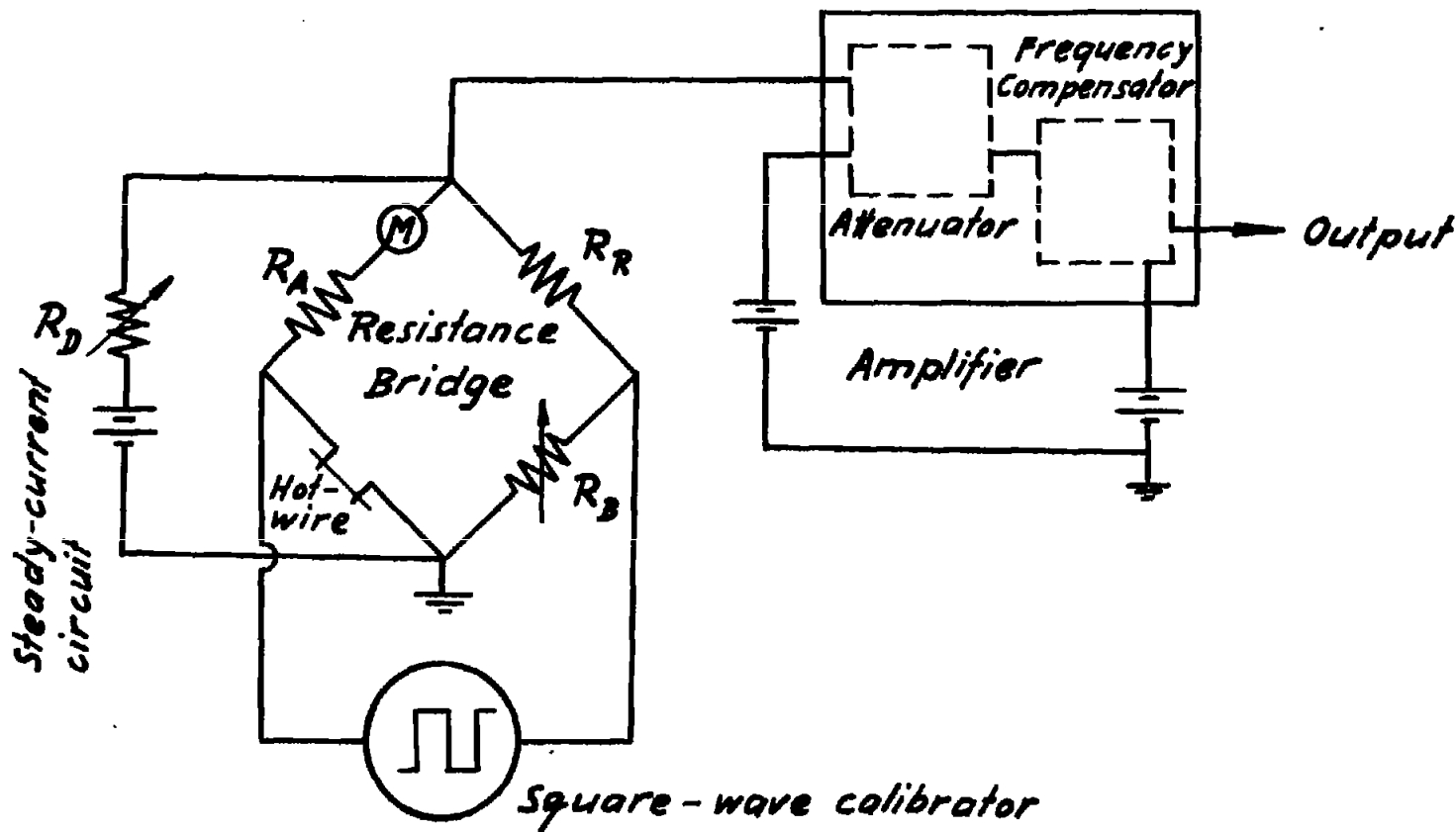
Figure 7.- Block diagram of Flow Corporation HWB unit. Labels indicate: R_R, resistance ratio switch; R_D, current controls; M, wire current meter; R_B, bridge null potentiometer.
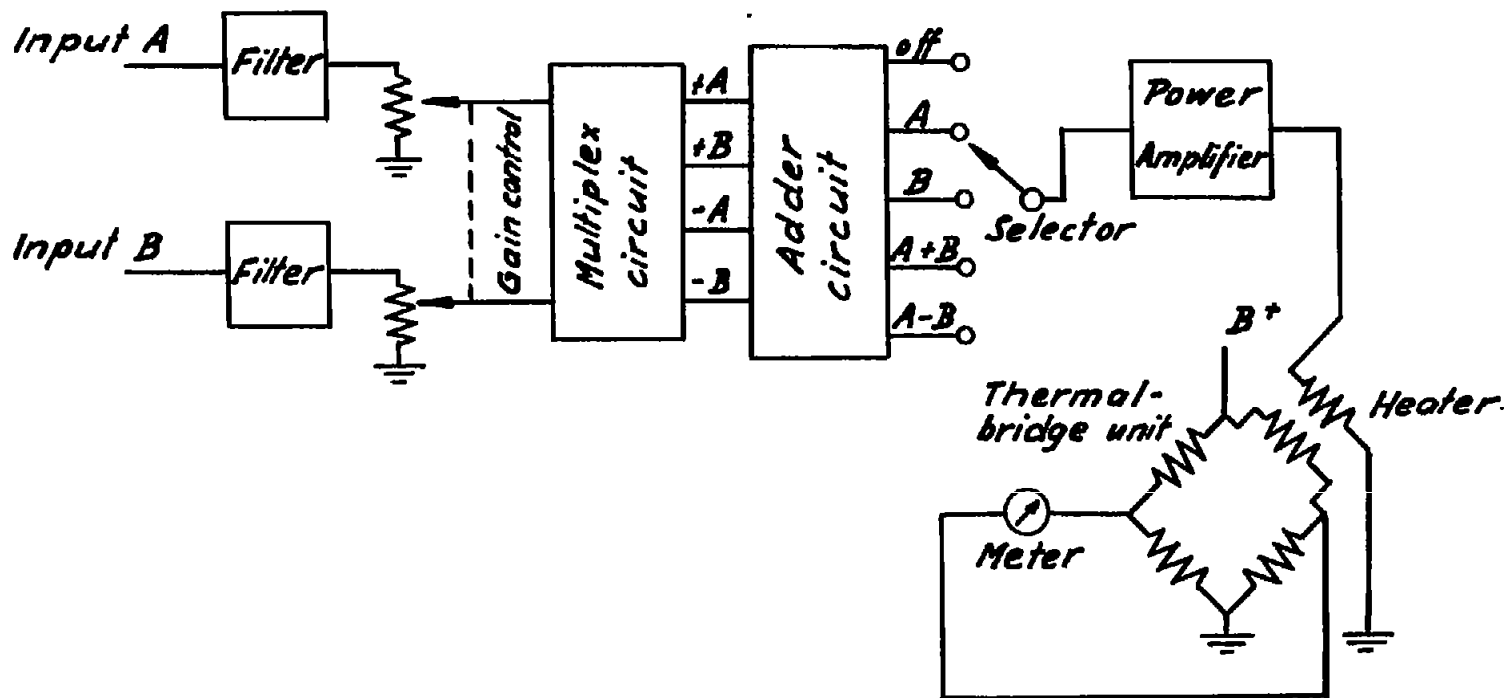
Figure 8.- Turbulence-unit block diagram.
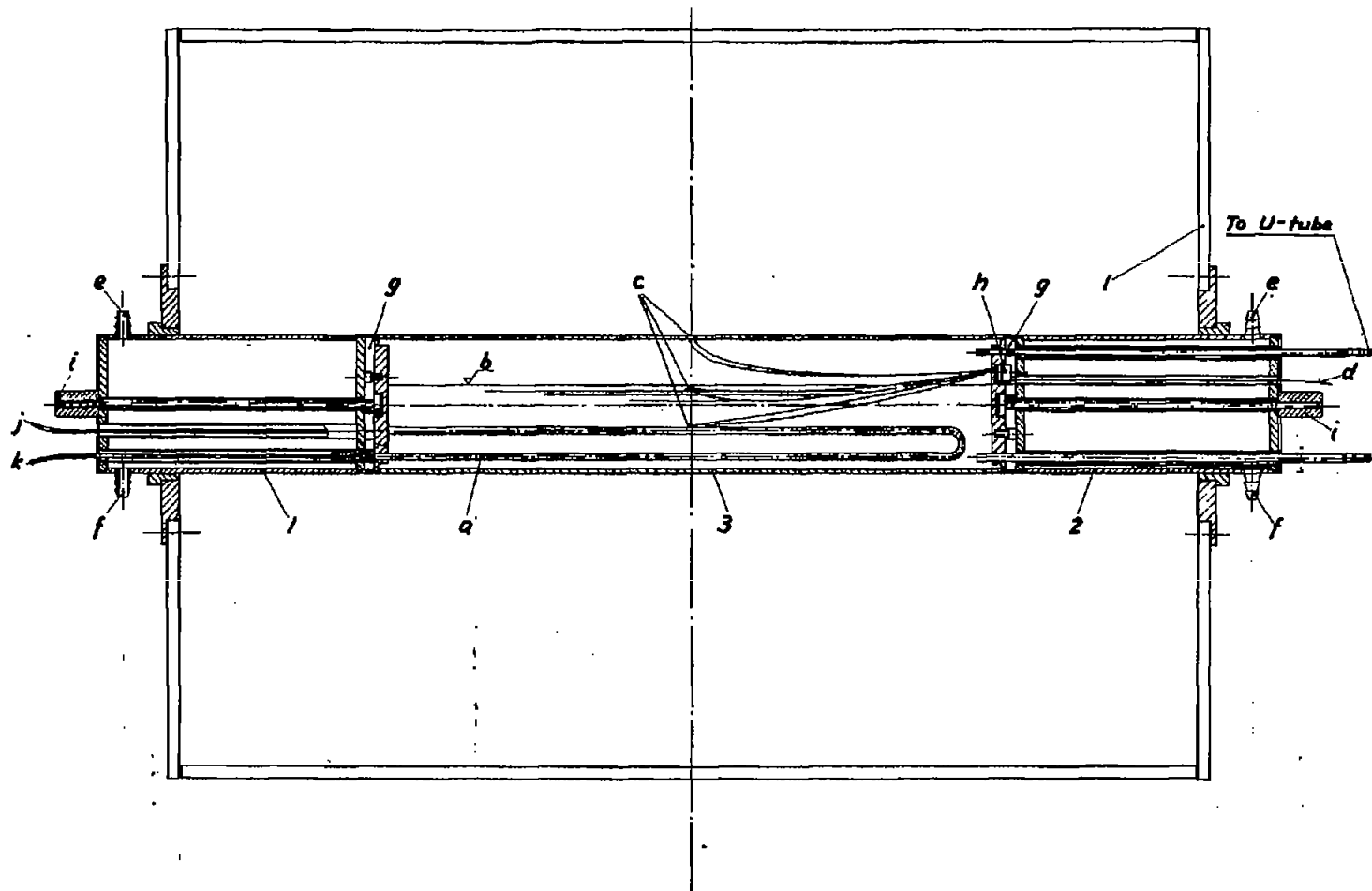
Figure 9.- Cross section of model tube. Labels indicate: a, electric heater; b, water level; c, thermocouples; d, thermocouples; e, steam inlet; f, steam outlet; g, insulation; h, thermocouple seal; i, tie-rods; j, supply of direct current; k, direct-current line; and l, test section.
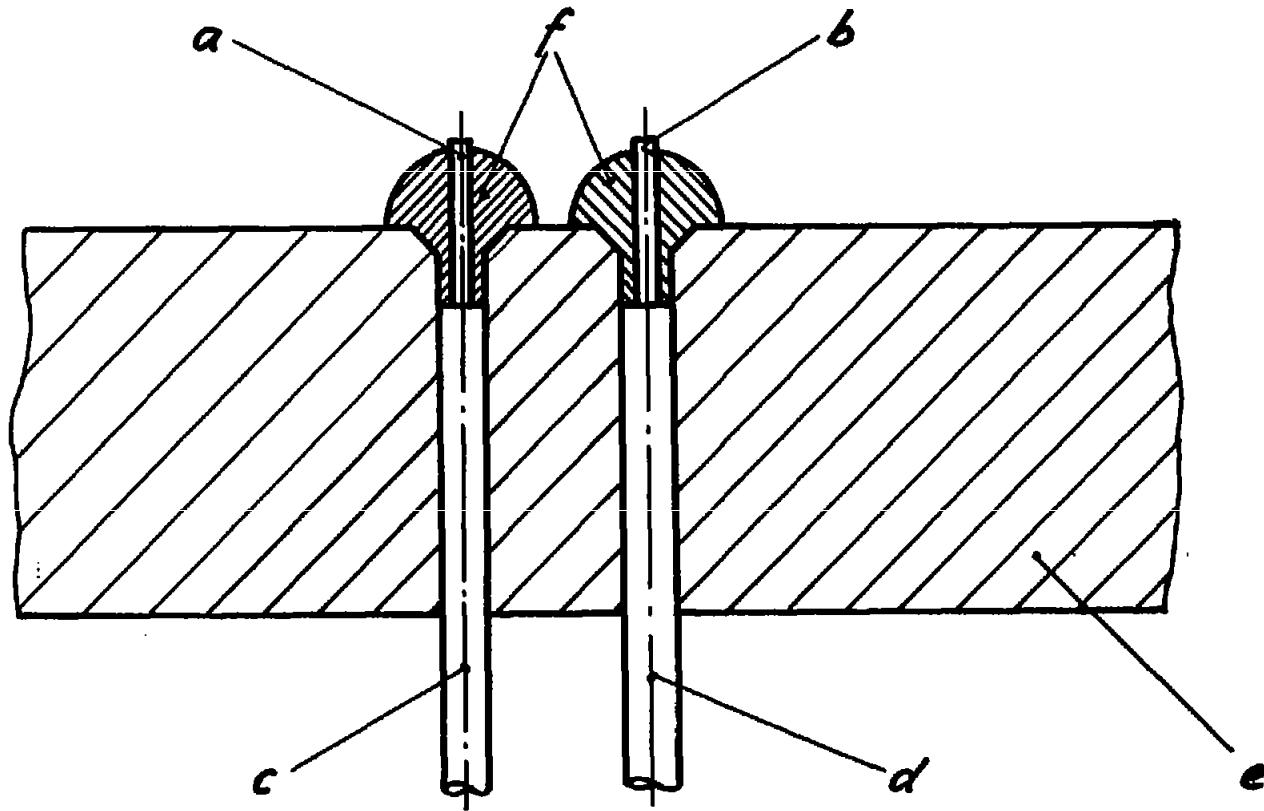
Figure 10.- Details of hot junction. Labels indicate: a, bared Chromel wire, 0.005-inch diameter;
   b, bared Alumel wire, 0.005-inch diameter; c, enameled Chromel wire, 0.0054-inch diameter;
   d, enameled Alumel wire, 0.0054-inch diameter; e, wall of brass tube; and f, solder, later
   polished off flush with wall.
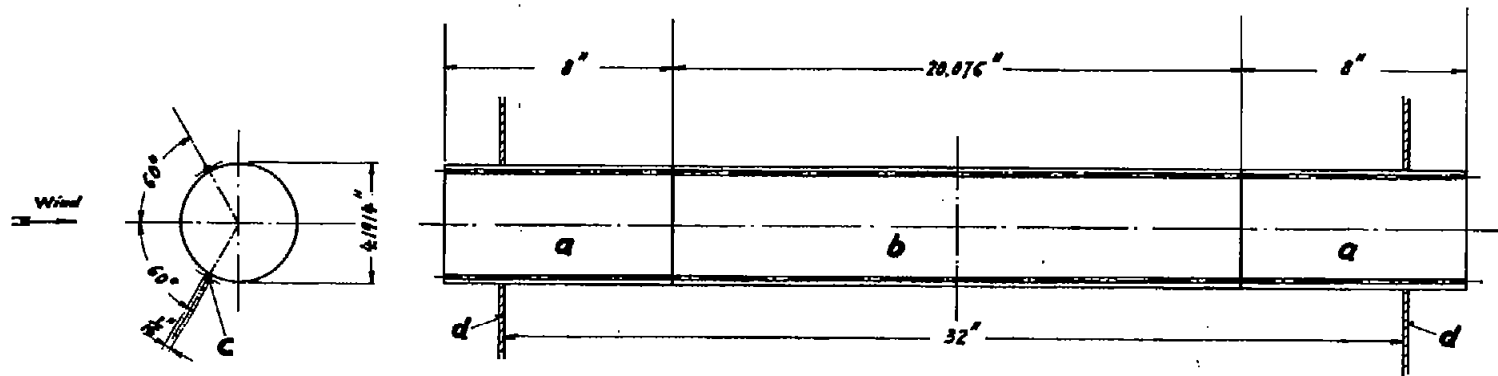
Figure 11.- Arrangement of tripping wires on test tube. Labels indicate: a, guard tube; b, test tube; c, tripping wire; and d, wind-tunnel wall.
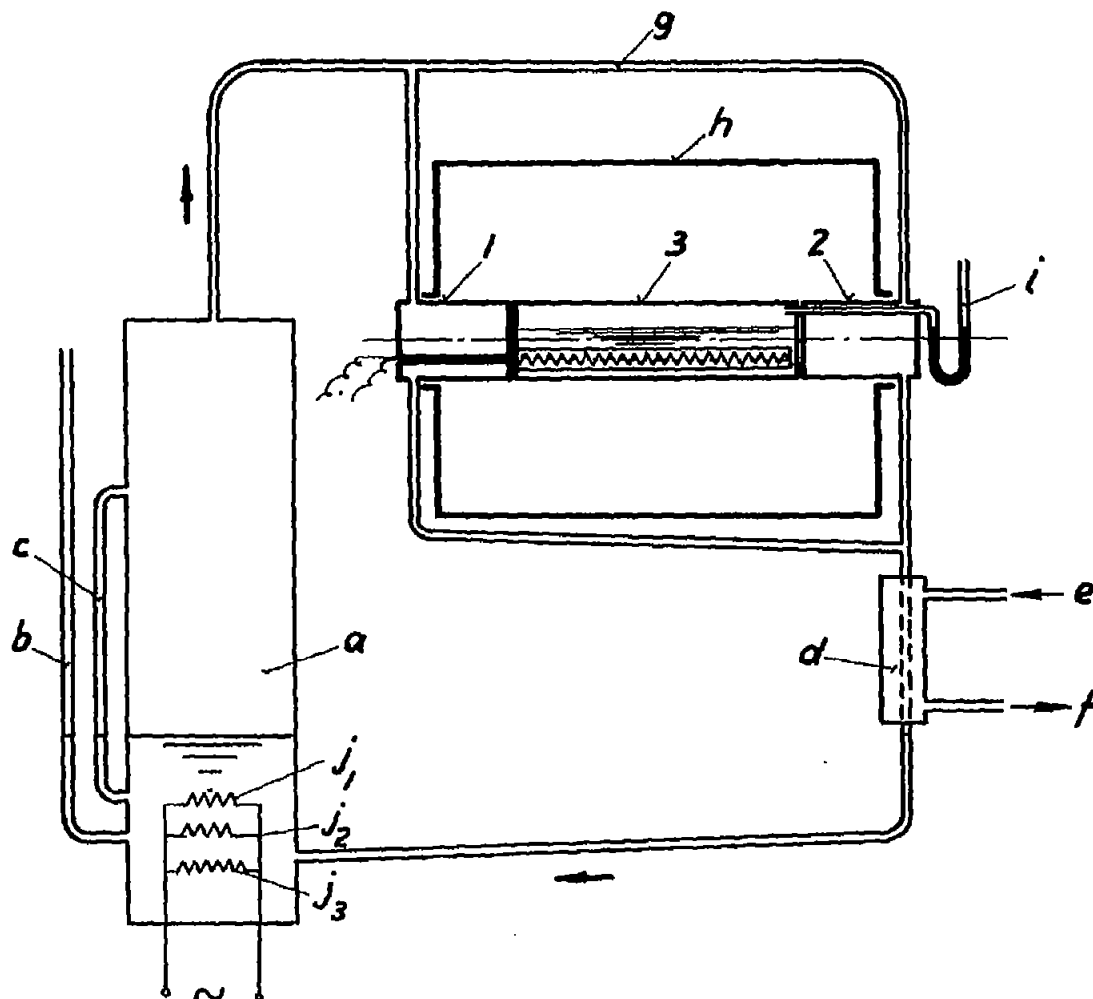
Figure 12.- Boiler and steam circulating system. Labels indicate: a, boiler; b, manometer;
c, water gauge; d, condenser; e, condenser inlet; f, condenser outlet; g, steam tubes; h, test
section; i, U tube; and j_1, j_2, and j_3, heaters.
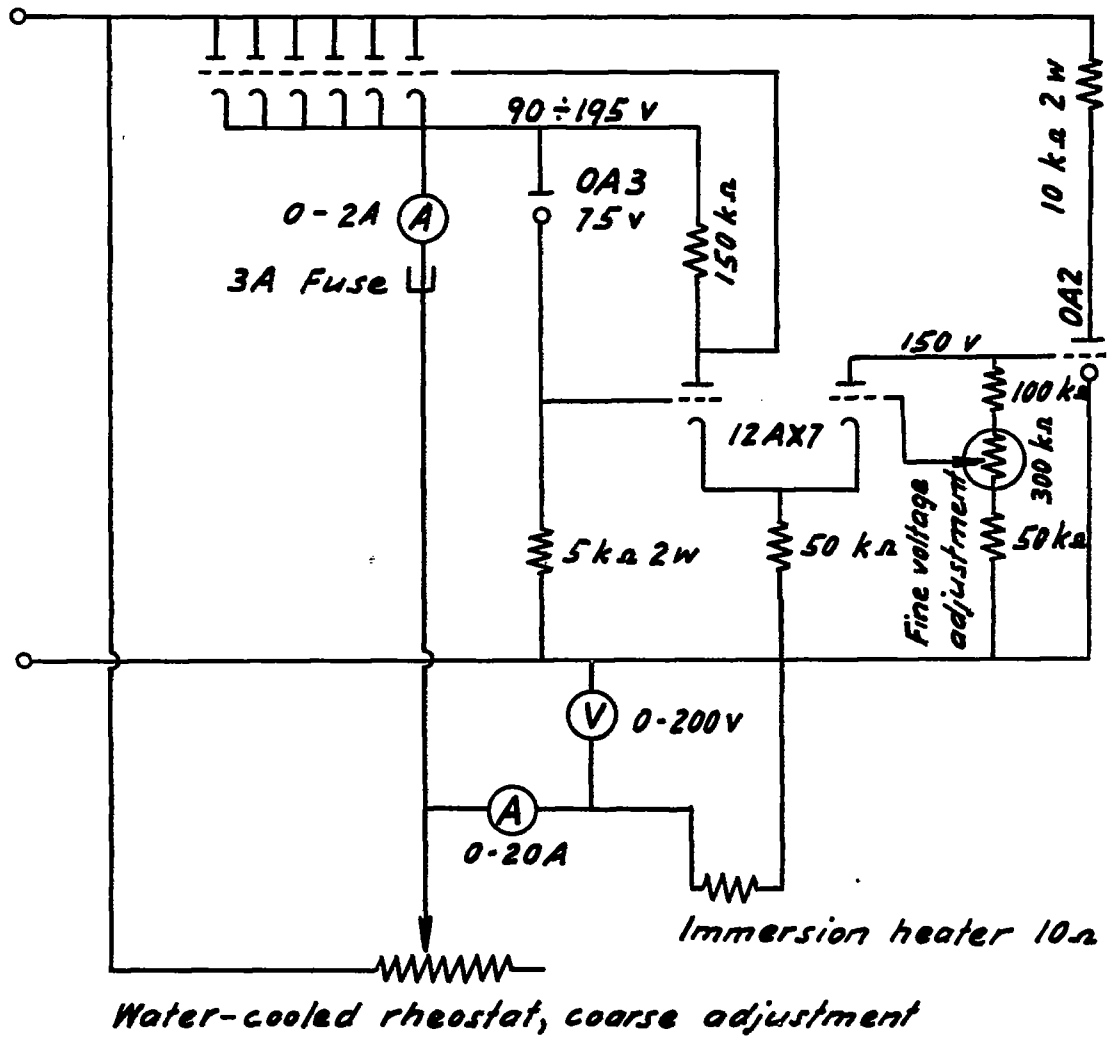
Figure 13.- Voltage-stabilizer circuit. Direct current of 230 volts from
rotary converter set.
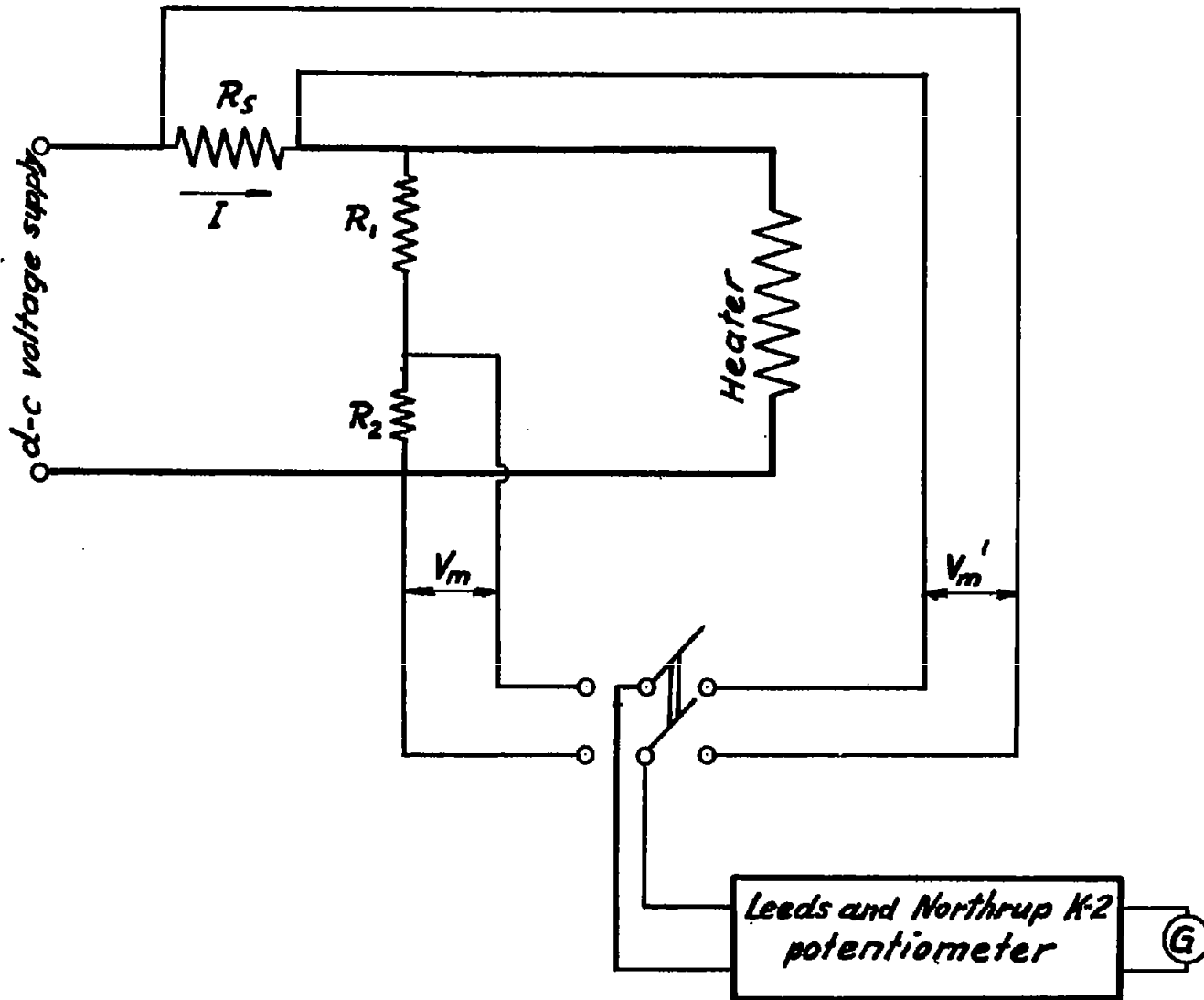
Figure 14.- Electrical measuring circuit.
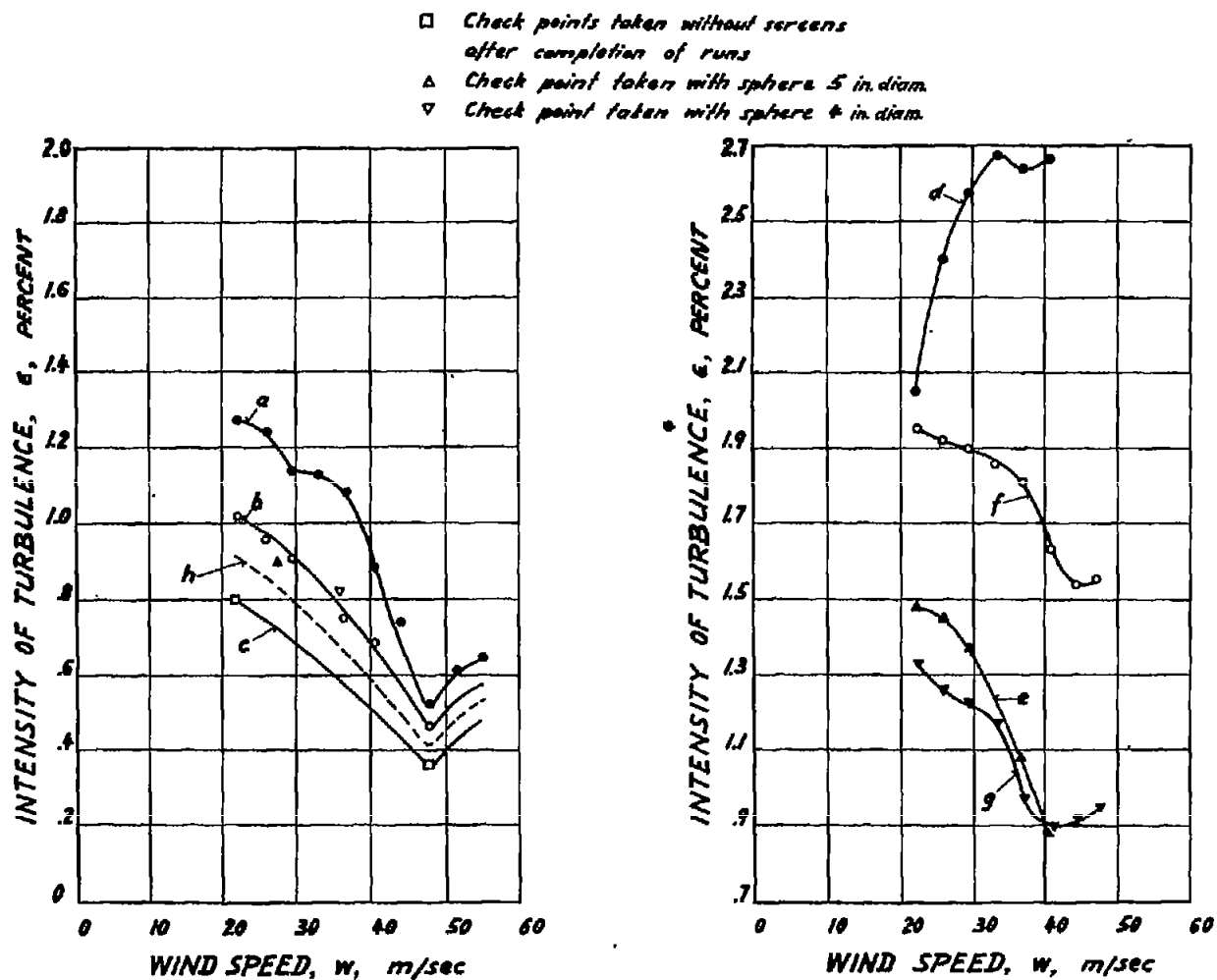
Figure 15.- Intensity of turbulence. Labels indicate: a, no screens, after vacuum cleaning; b, no screens, before test runs; c, no screens, after test runs; d, screen number 1 at 1 ft, run 2; e, screen number 1 at 2 ft, run 3; f, screen number 2 at 1 ft, run 4; g, screen number 2 at 2 ft, run 5; and h, curve interpolated from check points.
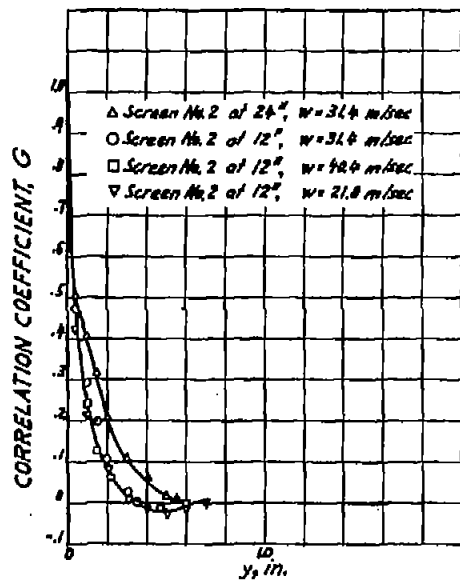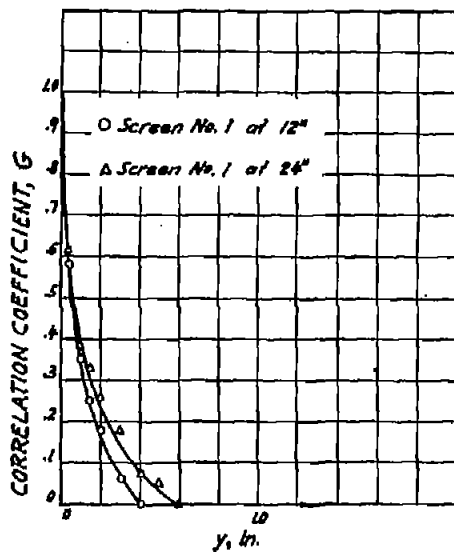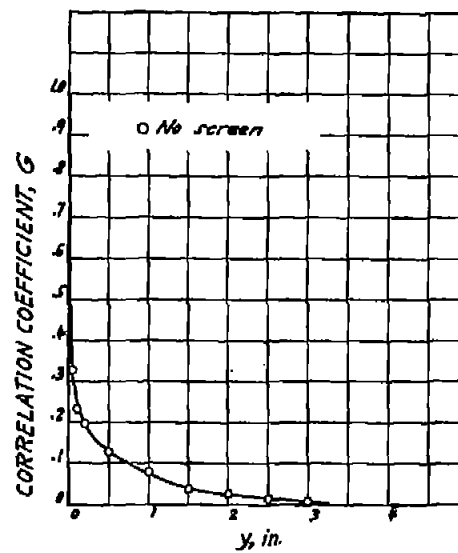
(a) Screen 2. (b) Screen 1. (c) No screen.

Figure 16.- Variation of correlation coefficient with probe separation.
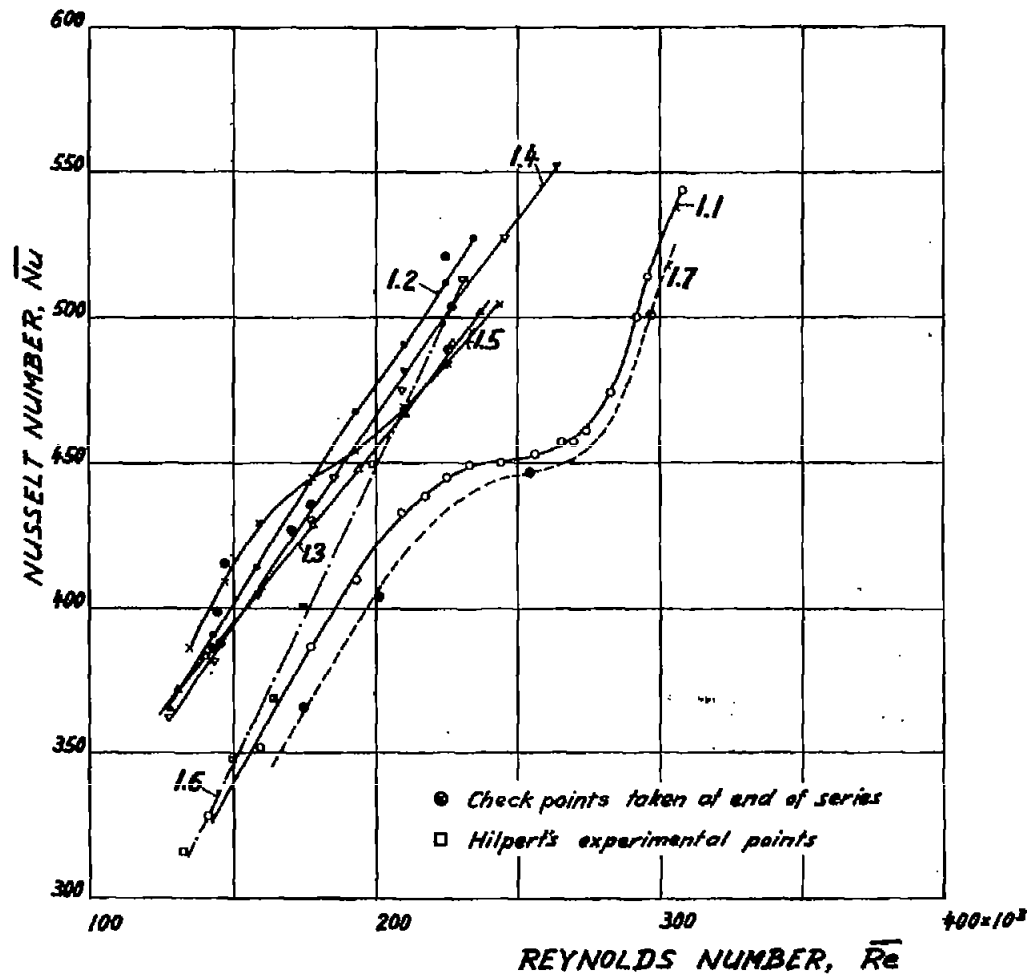
Figure 17.- Experimental results plotted as $\overline{Nu}$ versus $\overline{Re}$. Labels indicate: 1.1, no screen; 1.2, screen 1 (3/4 inch mesh) at 12 inches; 1.3, screen 1 at 24 inches; 1.4, screen 2 (1/2 inch mesh) at 12 inches; 1.5, screen 2 at 24 inches; 1.6, Hilpert's mean curve from equation (17); and 1.7, mean curve for low-turbulence measurements drawn through check points.
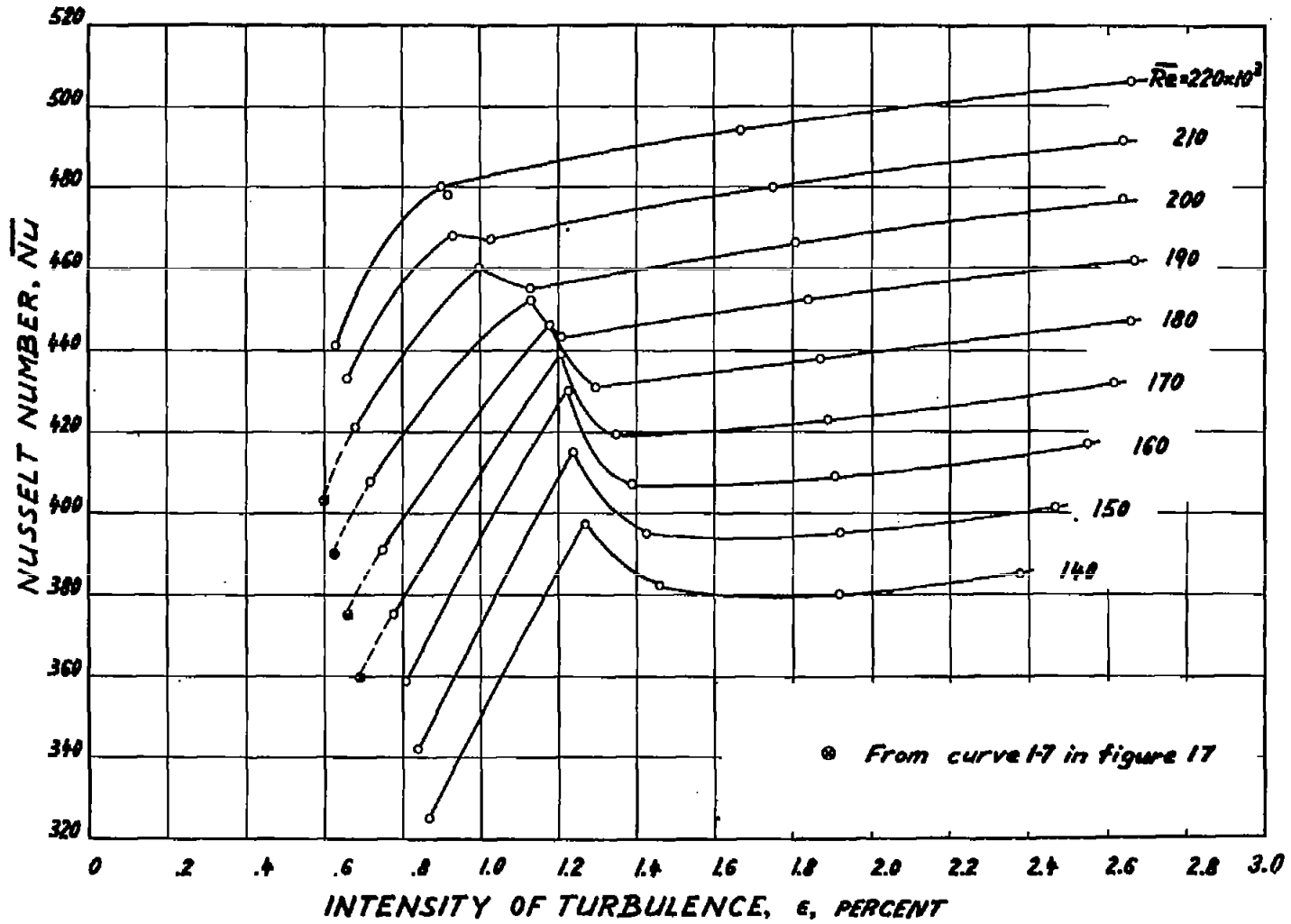
Figure 18.- Experimental results cross-plotted from figure 17. Variation of Nusselt number $\overline{\mathrm{Nu}}$ with intensity of turbulence ϵ at constant Reynolds number $\overline{\mathrm{Re}}$.
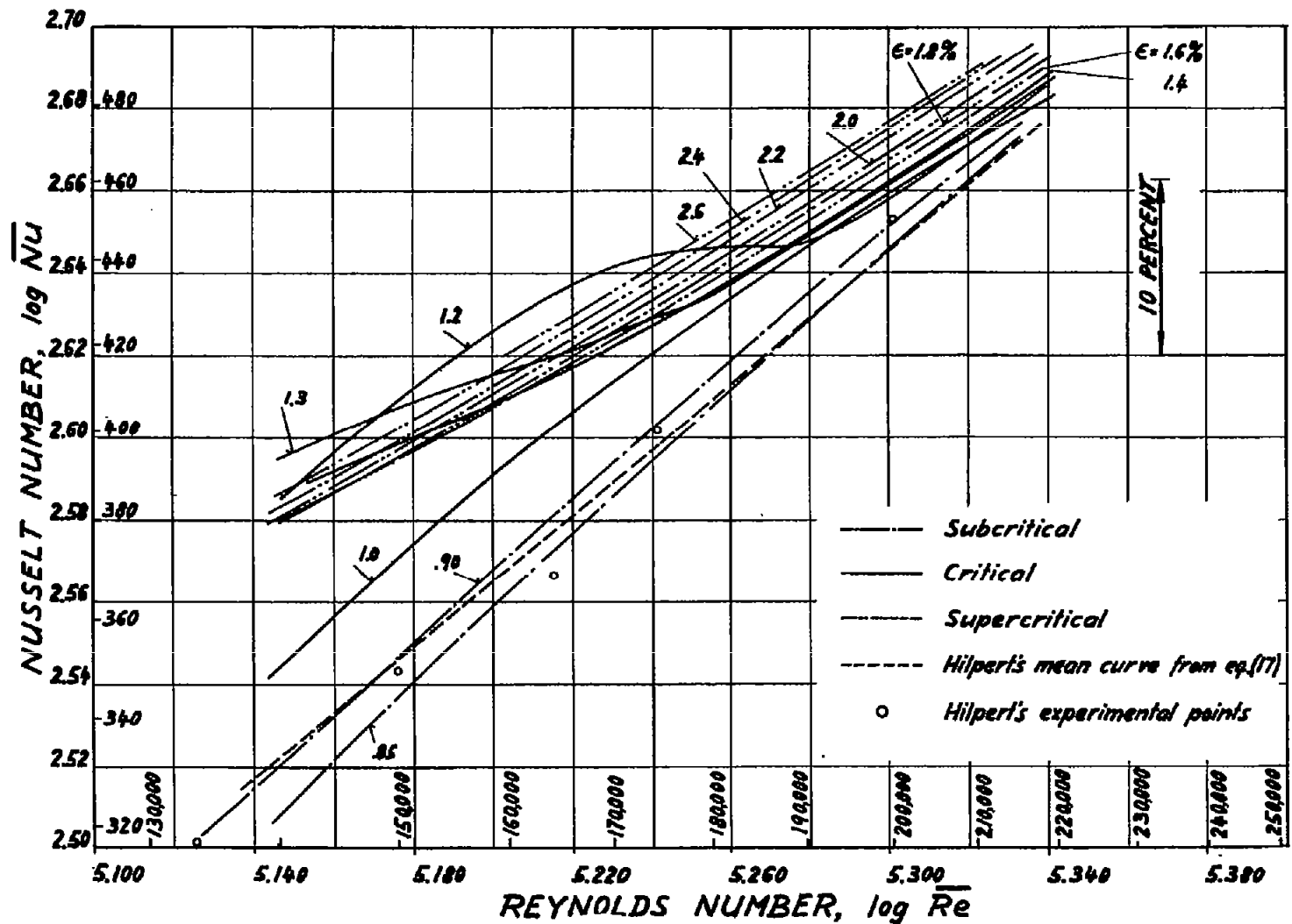
Figure 19.- Experimental results cross-plotted from figure 18. Variation of Nusselt number $\overline{Nu}$ with Reynolds number $\overline{Re}$ at constant intensity of turbulence ϵ.
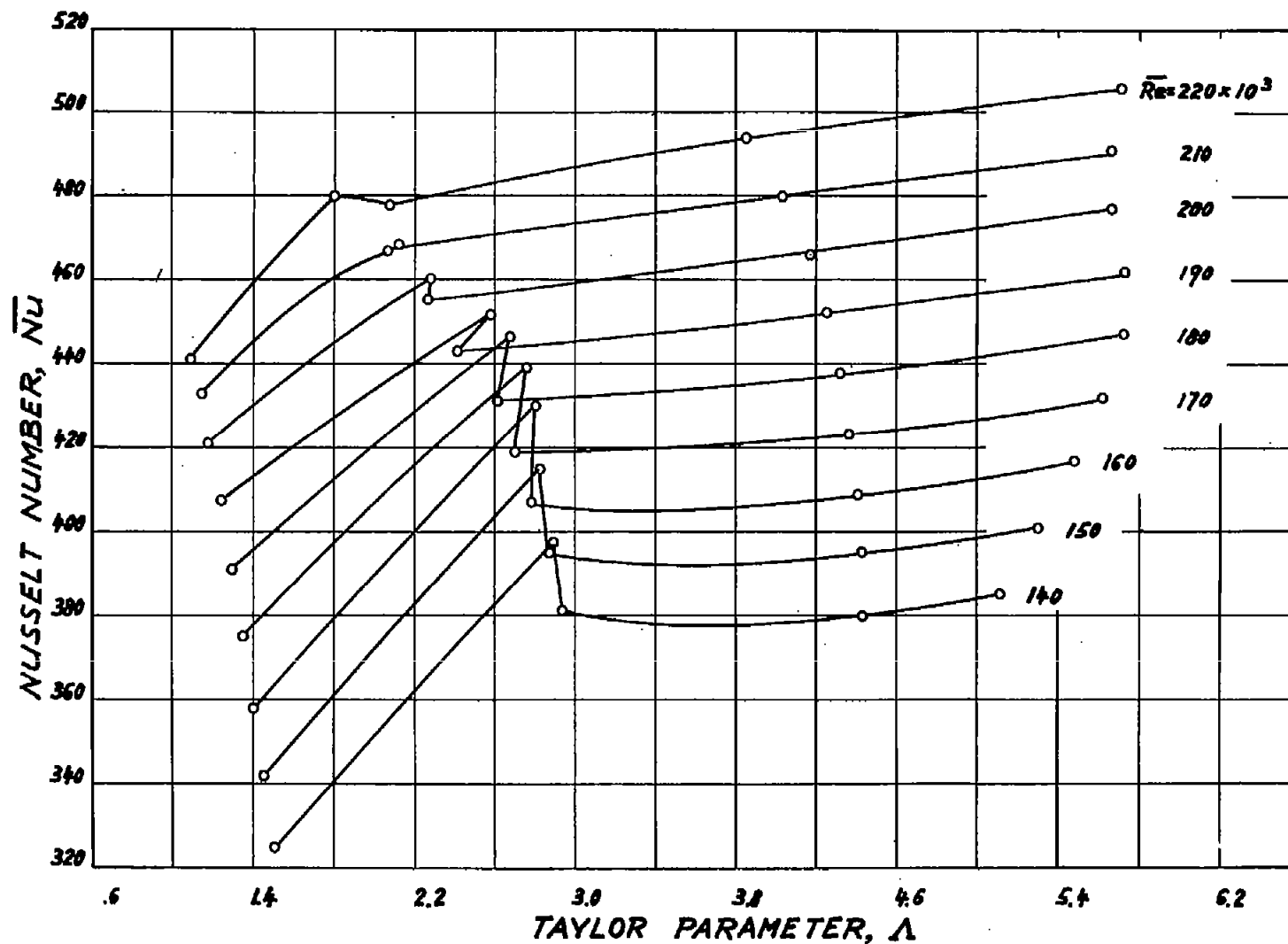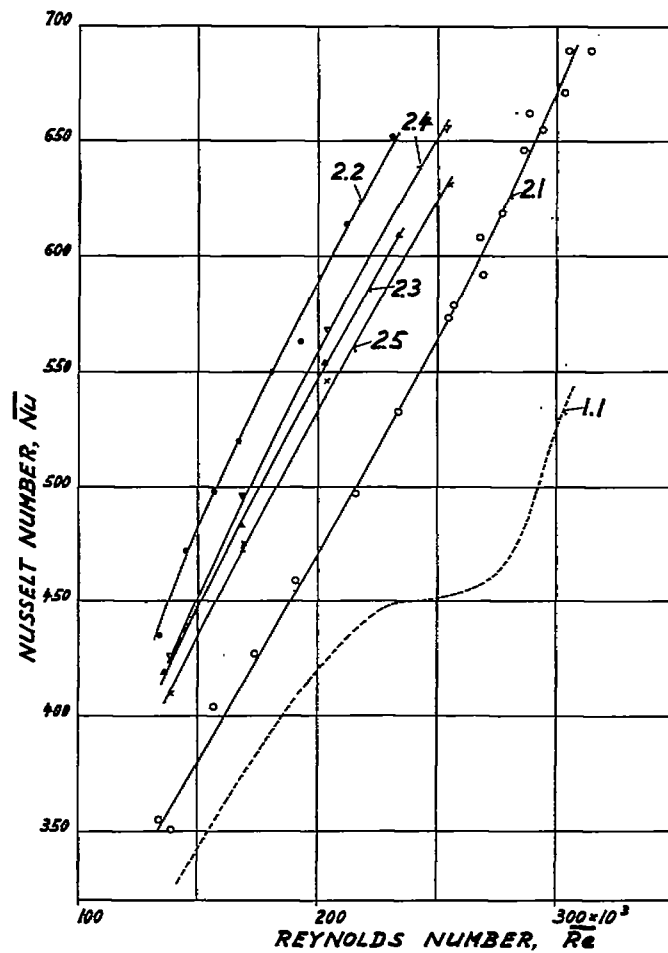
Figure 20.- Experimental results cross-plotted from figure 18. Variation of Nusselt number $\overline{Nu}$ with Taylor parameter Λ.
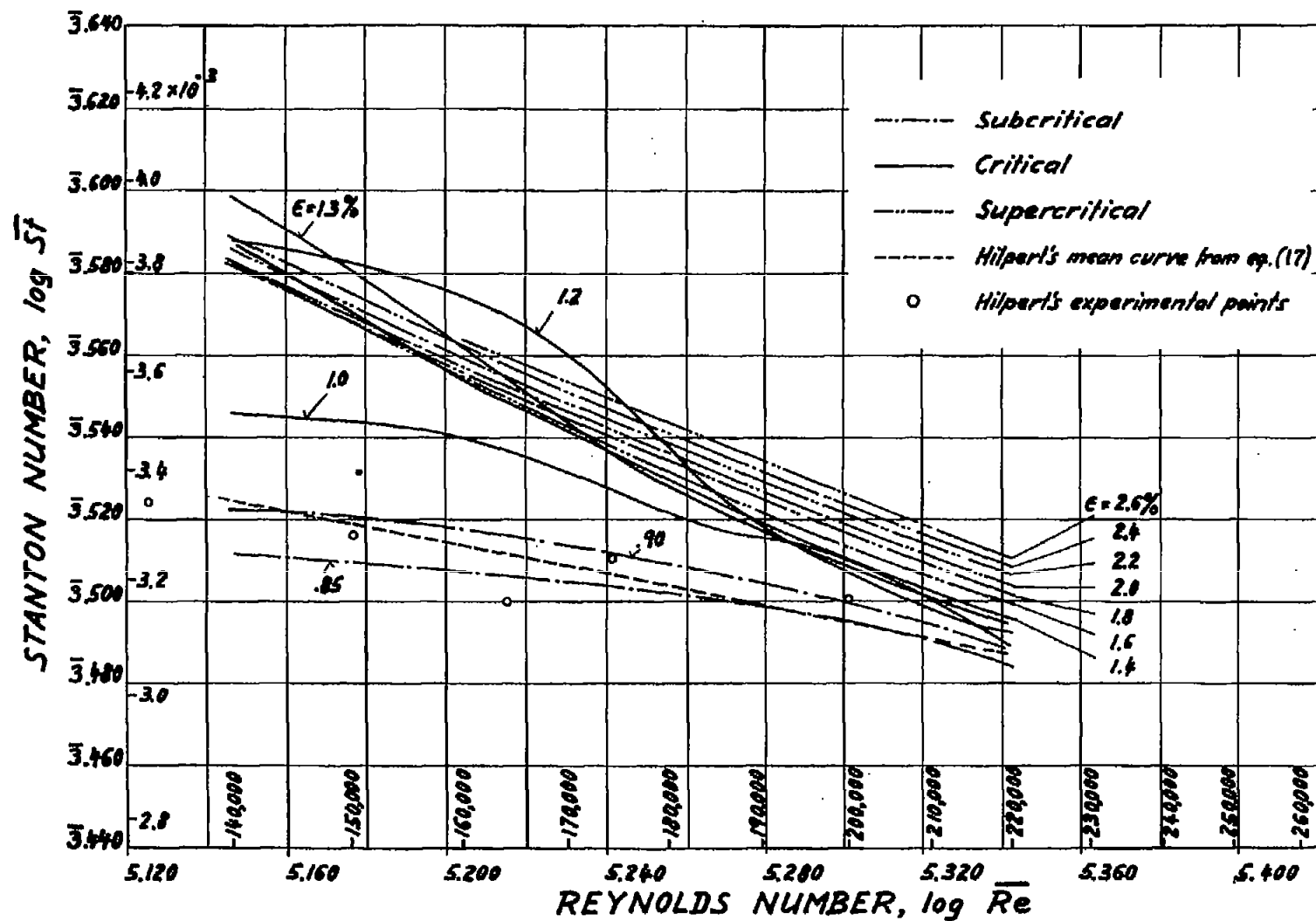
Figure 21.- Variation of Stanton number $\overline{St}$ in terms of Reynolds number $\overline{Re}$ at constant turbulence intensity ϵ. (Replot of fig. 19.)

Figure 22.- Experimental results plotted as $\overline{Nu}$ versus $\overline{Re}$. Labels indicate: 1.1, no screen, no tripping wires; 2.1, no screen; 2.2, screen at 12 inches; 2.3, screen at 24 inches; 2.4, screen at 12 inches; and 2.5, screen at 24 inches.
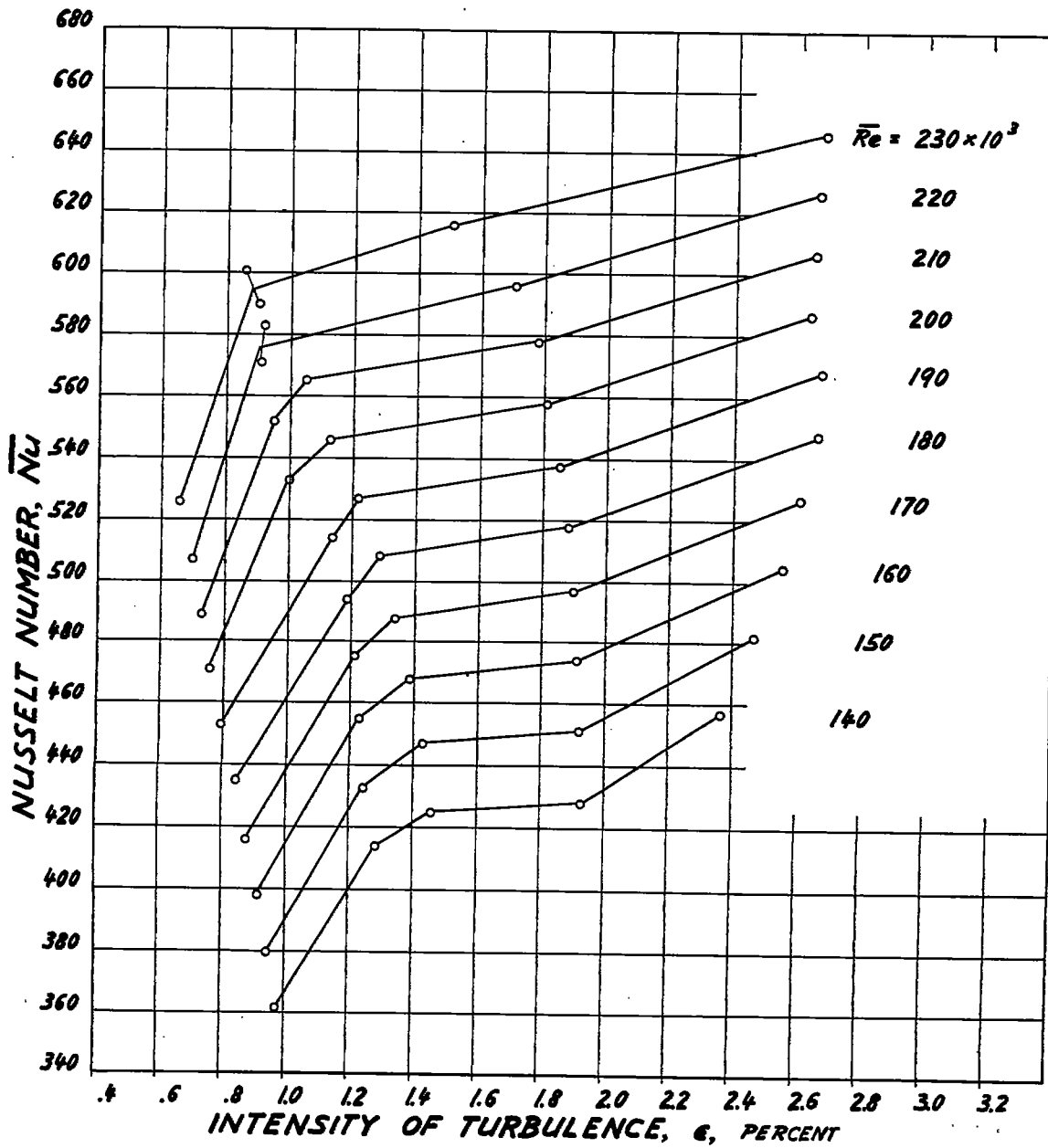
Figure 23.- Experimental results cross-plotted from figure 22. Variation
of Nusselt number $\overline{Nu}$ with intensity of turbulence ϵ at constant
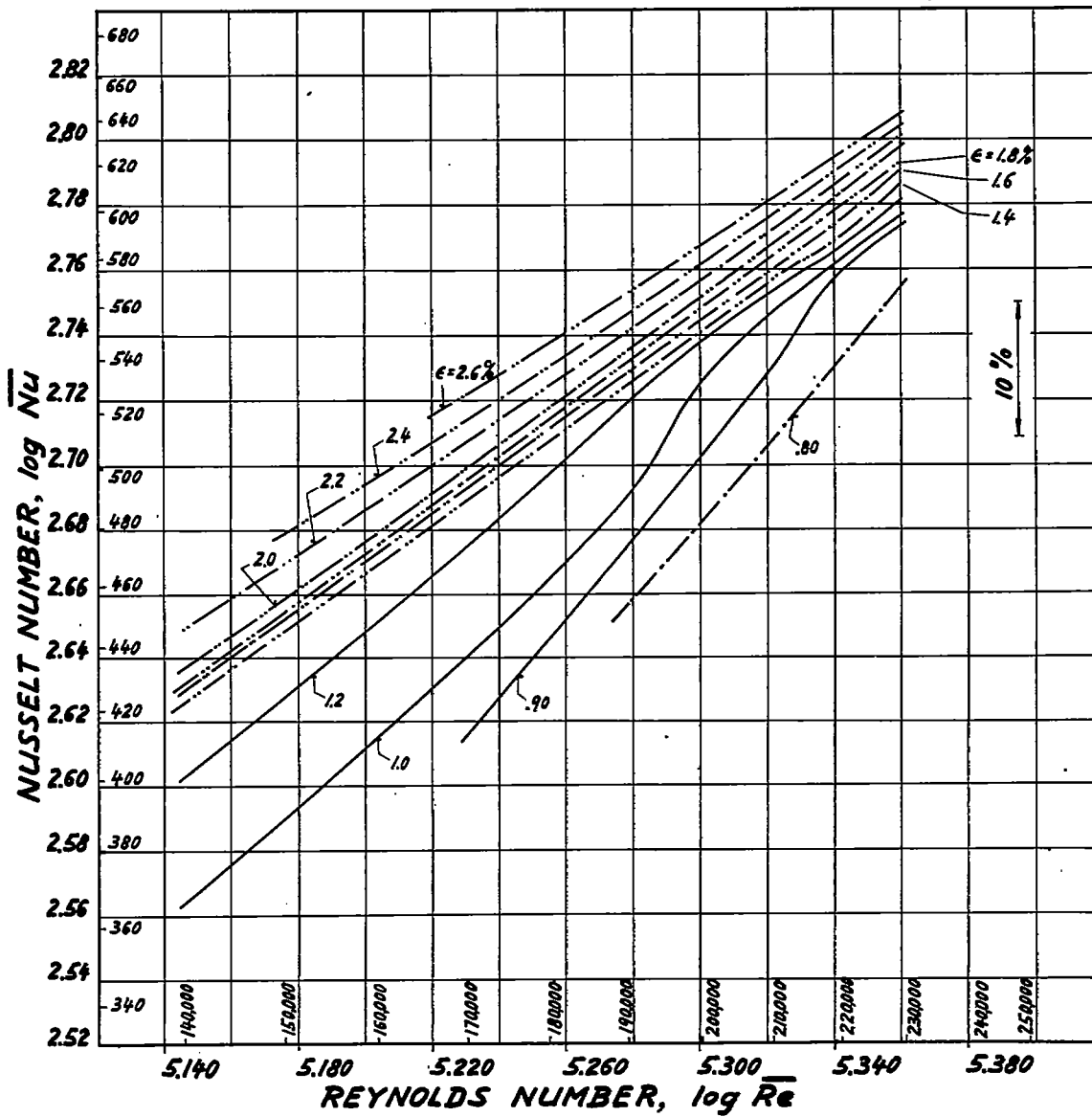Reynolds number $\overline{Re}$ (with tripping wires).

Figure 24.- Experimental results cross-plotted from figure 23. Variation
of Nusselt number $\overline{Nu}$ with Reynolds number $\overline{Re}$ at constant intensity
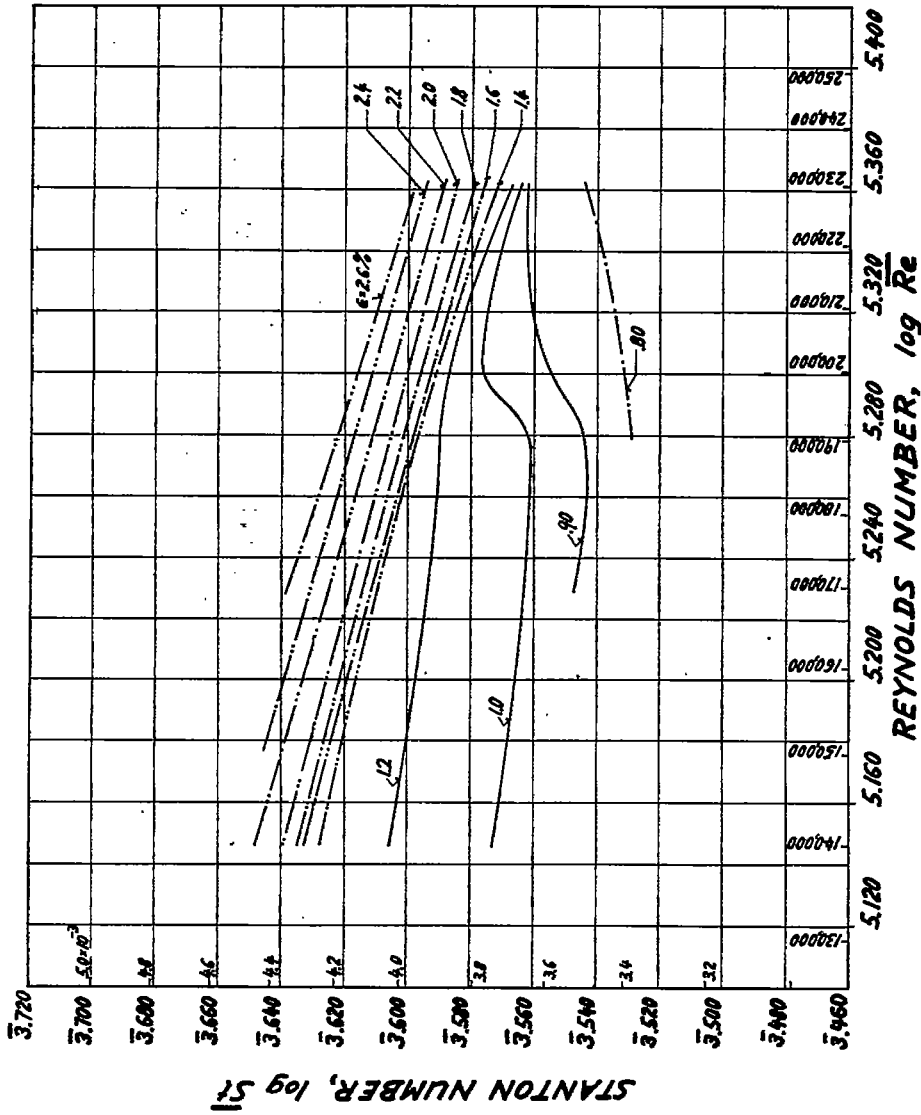of turbulence ϵ (with tripping wires).

Figure 25.- Variation of Stanton number $\overline{St}$ in terms of Reynolds number $\overline{Re}$ at constant intensity of turbulence ϵ (with tripping wires).